arXiv:2108.08355v2 [math.NA] 18 Oct 2021

AN EMA-CONSERVING, PRESSURE-ROBUST AND RE-SEMI-ROBUST RECONSTRUCTION METHOD FOR THE UNSTEADY INCOMPRESSIBLE NAVIER-STOKES EQUATIONS

XU LI AND HONGXING RUI

Abstract. Proper EMA-balance (E: kinetic energy; M: momentum; A: angular momentum), pressure-robustness and *Re*-semi-robustness (*Re*: Reynolds number) are three important properties of Navier-Stokes simulations with exactly divergence-free elements. This EMA-balance makes a method conserve kinetic energy, linear momentum and angular momentum under some suitable senses; pressure-robustness means that the velocity errors are independent of the continuous pressure; *Re*-semi-robustness means that the constants appearing in the error bounds of kinetic and dissipation energies do not explicitly depend on inverse powers of the viscosity. In this paper, based on the pressure-robust reconstruction methods in [A. Linke and C. Merdon, *Comput. Methods Appl. Mech. Engrg.* 311 (2016), 304-326], we propose a novel reconstruction method for a class of non-divergence-free simplicial elements which admits almost all the above properties. The only exception is the energy balance, where kinetic energy should be replaced by a properly redefined discrete energy. Some numerical comparisons with exactly divergence-free methods, pressure-robust reconstructions and the EMAC scheme are provided to confirm our theoretical results.

1. Introduction

In this paper, we study the finite element methods for the unsteady Navier-Stokes equations (NSEs):

$$\boldsymbol{u}_t - \nu\Delta\boldsymbol{u} + (\boldsymbol{u}\cdot\nabla)\,\boldsymbol{u} + \nabla p = \boldsymbol{f} \qquad \text{in } J\times\Omega, \tag{1.1a}$$

$$\nabla\cdot\boldsymbol{u} = 0 \qquad \text{in } J\times\Omega, \tag{1.1b}$$

$$\boldsymbol{u}(0) = \boldsymbol{u}^0 \qquad \text{in } \Omega, \tag{1.1c}$$

$$\boldsymbol{u} = \boldsymbol{0} \qquad \text{on } J\times\Gamma, \tag{1.1d}$$

where $J = (0,T]$ and $\Omega \subset \mathbb{R}^d$ $(d = 2,3)$ is a bounded domain with Lipschitz-continuous polyhedral boundary Γ; $\boldsymbol{u}$ and p represent the unknown velocity and pressure, respectively; $\nu > 0$ is the constant kinematic viscosity; $\boldsymbol{f}$ represents the external force and $\boldsymbol{u}^0$ is the initial velocity. We assume $\boldsymbol{f}(t) \in \boldsymbol{L}^2(\Omega)$ for all $t \in J$. For simplicity, here we only consider the homogeneous Dirichlet boundary condition. Other boundary conditions are also of interest.

2020 *Mathematics Subject Classification.* 65M12, 65M15, 65M60, 76D05, 76D17.

Key words and phrases. Finite element methods, unsteady Navier-Stokes equations, pressure-robustness, EMAC formulation, *Re*-semi-robustness.

The second author is the corresponding author.

This work was supported by the National Natural Science Foundation of China grant 12131014.

For designing accurate numerical schemes, it is widely believed that preserving the fundamental (physical or mathematical) properties of the continuous problem is of great importance. For the unsteady incompressible Navier-Stokes equations, these fundamental properties include the divergence constraint (1.1b), the balance laws for some physical quantities (e.g., kinetic energy, linear momentum, angular momentum, vorticity, helicity and enstrophy) [10, 18], an invariance property for the velocity with respect to the gradient field in $\boldsymbol{f}$ [30, 35] and so on. Among these properties, the divergence constraint is of central importance. The papers [18, 30] respectively showed that the exactly divergence-free mixed methods preserved the balance laws and the invariance property mentioned above. The latter means that these methods are pressure-robust; namely the velocity errors are independent of the pressure. Moreover, it was demonstrated in [46] that the constants in error estimates, including the Gronwall constant, did not depend on ν^{-1} explicitly for divergence-free finite element methods. This property was called (Re-)semi-robustness, uniform, or quasi-uniform estimates [29] sometimes.

Due to these fascinating properties, constructing exactly divergence-free elements has been an increasingly hot topic in recent years [12, 25–27, 39, 40, 49]. However, compared to classical non-divergence-free elements (e.g., Taylor-Hood, MINI and Bernardi-Raugel, cf. [23, 28]), the construction of these elements is not trivial in most cases. Another popular idea is relaxing the continuity condition but enforcing the divergence constraint strongly, which results in the so-called nonconforming $H(\mathrm{div})$-conforming methods [14, 24, 31, 45, 47, 48]. In this paper, we focus on the conforming mixed methods for the Navier-Stokes equations.

Modifying the formulation to preserve some fundamental properties of the continuous problem (or divergence-free mixed methods) for non-divergence-free elements is another popular research topic. With an observation that most classical elements are non-divergence-free, this topic includes (not just) pressure-robust reconstructions [32, 34–37], the EMAC (EMA-conserving) formulation [10, 11, 42] and some Re-semi-robust methods [8, 15, 16, 20]. The method introduced in this paper is also included in this topic. Pressure-robustness plays an important role on the accuracy of a method when *'gradient forces dominate the momentum balance'* [38]; the velocity errors of the methods which are not Re-semi-robust might grow quickly with respect to time for higher Reynolds number flows [46]; the EMAC scheme is one of the "enhanced-physics" based schemes which have a long history such as [1, 2, 19, 43, 44], and the paper [42] showed that an improper treatment of energy, linear momentum and angular momentum produced lower bounds for L^2 velocity errors. It is worth mentioning that, the properties mentioned above are usually not mutually independent. For example, in the paper [42], Olshanskii and Rebholz proved that the Gronwall constants in EMAC estimates did not depend on the viscosity explicitly, which is exactly Re-semi-robustness except that the constant in the pressure-induced error polynomially depended on the inverse of viscosity. Another example is the popular grad-div stabilization [9, 41]. It can not only weaken (not totally remove) the impact of the pressure on velocity errors [30] but also make the usual skew-symmetric scheme semi-robust with respect to the Reynolds number [15]. Finally, we also refer the readers to the review article [29] for more details.

In this paper, we propose a novel reconstruction formulation which is EMA-conserving for the reconstructed discrete velocity (here the energy should be re-defined), pressure-robust and Re-semi-robust. For simplicity, we shall refer to this reconstruction as the "EMAPR" reconstruction throughout this paper. Our method is based on the pressure-robust reconstruction formulation in [37]. The main difference lies on the discretization of the convective term. For the convective term, two (pressure-robust) discrete forms were proposed in [37]: the convective form and the rotational form. Similarly to [10], it can be checked that the two forms do not conserve the linear momentum and angular momentum (the latter conserves kinetic energy). Here we propose an EMA-conserving form, i.e., it does not produce any extra energy, momentum and angular momentum under some appropriate senses. Then we give a pressure-robust and Re-semi-robust error estimate for the continuous-in-time case, provided that the continuous solution $\boldsymbol{u}$ is in $L^2\left(J;\boldsymbol{W}^{1,\infty}(\Omega)\right)$. To obtain such an estimate, we also need to slightly modify the discretization of the evolutionary term by introducing a stabilization. Finally, we shall prove that our formulation could be easily applied to a class of simplicial locally mass-conserving elements whose pressures are discontinuous. To the best of our knowledge, the EMAPR reconstruction is the first method on conforming non-divergence-free elements which is EMA-conserving, pressure-robust and Re-semi-robust simultaneously. For nonconforming and non-divergence-free methods, a reconstructed Hybrid discontinuous Galerkin method in [33] (see formulas "(6.3d)" and "(6.5)" in it) probably admits most of these properties also.

The remainder of this paper is organized as follows. In Section 2 we discuss the EMAPR methods and some balance laws. Section 3 is devoted to giving a pressure-robust and Re-semi-robust error estimate for the EMAPR method. We show that a class of locally divergence-free elements (include the Bernardi-Raugel element) could be easily incorporated into our framework in Section 4. Finally we carry out some numerical experiments in Section 5.

In what follows we will use C, with or without a subscript, to denote a generic positive constant. The standard inner product for $\left[L^2(D)\right]^n$ or $\left[L^2(D)\right]^{n\times n}$ ($n\in\mathbb{Z}$) will be denoted by $(\cdot,\cdot)_D$ uniformly. The notation $\|\cdot\|_{m,p,D}$ ($|\cdot|_{m,p,D}$) will be used to denote the Sobolev norm (seminorm, respectively) of $[W^{m,p}(D)]^n$ or $[W^{m,p}(D)]^{n\times n}$. With the convention the subscripts m,p and D will be omitted for $m=0$, $p=2$ and $D=\Omega$, respectively. $H^m(D)$ coincides with $W^{m,2}(D)$ and $\boldsymbol{W}^{m,p}(D)$ coincides with $[W^{m,p}(D)]^d$.

2. The EMAPR reconstruction method

2.1. **The divergence-free reconstruction operator.** Let $\mathcal{T}_h$ denote a partition of Ω. We define the mesh size $h:=\max_{K\in\mathcal{T}_h}h_K$ with h_K the diameter of elements K. Denote by ϱ_K the diameter of the biggest ball inscribed in K. Here we assume that $\mathcal{T}_h$ is shape-regular [13], i.e., there exists a positive constant ξ such that

$$\frac{h_K}{\varrho_K}\leq\xi\quad\forall\ K\in\mathcal{T}_h. \tag{2.1}$$

Introduce

$$\begin{aligned}
V=\boldsymbol{H}_0^1(\Omega)&:=\left\{\boldsymbol{v}\in\boldsymbol{H}^1(\Omega):\boldsymbol{v}|_\Gamma=\boldsymbol{0}\right\},\\
X=\boldsymbol{H}_0(\mathrm{div};\Omega)&:=\{\boldsymbol{v}\in\boldsymbol{H}(\mathrm{div};\Omega):\boldsymbol{v}\cdot\boldsymbol{n}|_\Gamma=0\},\\
\boldsymbol{H}^2(\mathcal{T}_h)&:=\left\{\boldsymbol{v}\in\boldsymbol{L}^2(\Omega):\boldsymbol{v}|_K\in\boldsymbol{H}^2(K)\quad\forall\ K\in\mathcal{T}_h\right\},
\end{aligned}$$

and

$$W = L_0^2(\Omega) := \left\{ q \in L^2(\Omega) : \int_\Omega q \, d\boldsymbol{x} = 0 \right\},$$

where $\boldsymbol{n}$ is the unit external normal vector on Γ. Furthermore we define the bilinear form $b : X \times W \to \mathbb{R}$ by

$$b(\boldsymbol{v}, q) := (\nabla \cdot \boldsymbol{v}, q) \quad \text{for any} \quad (\boldsymbol{v}, q) \in X \times W.$$

Let $(V_h, X_h, W_h) \subset (V, X, W)$ denotes a triple of finite element spaces satisfying

$$\inf_{q_h \in W_h} \sup_{\boldsymbol{v}_h \in V_h \setminus \{\boldsymbol{0}\}} \frac{b(\boldsymbol{v}_h, q_h)}{\|\nabla \boldsymbol{v}\|} \geq \beta_h \|q_h\| \text{ for some } \beta_h > 0, \tag{2.2}$$

and

$$\nabla \cdot X_h \subseteq W_h. \tag{2.3}$$

Remark 1. For simplicity, throughout this article we assume that $\boldsymbol{u} \notin V_h$ for the true solution $\boldsymbol{u}$. This assumption does not influence the construction of the method, but will be beneficial to simplifying notation in error estimates and highlighting the fundamental ideas. For a more general velocity, there is no extra essential difficulty for analysis.

Denote by

$$V^0 := \{ \boldsymbol{v} \in V : b(\boldsymbol{v}, q) = 0 \quad \forall\, q \in W \} = \{ \boldsymbol{v} \in V : \nabla \cdot \boldsymbol{v} = 0 \},$$

and

$$V_h^0 := \{ \boldsymbol{v}_h \in V_h : b(\boldsymbol{v}_h, q_h) = 0 \quad \forall\, q_h \in W_h \},$$

the spaces of divergence-free velocity functions and discretely divergence-free velocity functions, respectively. Note that if $\nabla \cdot V_h \subseteq W_h$, we have $V_h^0 \subset V^0$, which means that the functions in V_h^0 are exactly divergence-free. For most classical elements, this relationship does not hold.

Let $P^k(K)$ denotes the space of polynomials on K of degree no more than k. We also define

$$\boldsymbol{P}^k := \left\{ \boldsymbol{v}_h \in V : \boldsymbol{v}_h|_K \in \left[P^k(K)\right]^d \text{ for all } K \in \mathcal{T}_h \right\}.$$

We suppose that the velocity space V_h is of order k ($k \geq 1$), i.e., there exists a non-negative integer k such that $\boldsymbol{P}^k \subset V_h$ and $\boldsymbol{P}^{k+1} \not\subset V_h$.

We introduce the divergence-free reconstruction operator $\Pi_h : V_h \to X_h$ (we do not give the concrete definition here) which satisfies that

$$\nabla \cdot \Pi_h \boldsymbol{v}_h \equiv 0 \text{ for all } \boldsymbol{v}_h \in V_h^0; \tag{2.4}$$

$$b(\boldsymbol{v}_h, q_h) = b(\Pi_h \boldsymbol{v}_h, q_h) \text{ for all } (\boldsymbol{v}_h, q_h) \in V_h \times W_h; \tag{2.5}$$

$$(\boldsymbol{g}, \boldsymbol{v}_h - \Pi_h \boldsymbol{v}_h) \leq C h^k |\boldsymbol{g}|_{k-1} \|\nabla \boldsymbol{v}_h\| \text{ for all } \boldsymbol{g} \in \boldsymbol{H}^{k-1}(\Omega), \boldsymbol{v}_h \in V_h^0. \tag{2.6}$$

Note that (2.4) can be derived from (2.3) and (2.5).

We also assume that Π_h satisfies the following properties.

Assumption 1. *There exists two operators $\Pi_h^1 : V_h \to V_h$ and $\Pi_h^R : V_h \to X_h$ such that $\Pi_h \boldsymbol{v} = \Pi_h^1 \boldsymbol{v} + \Pi_h^R \boldsymbol{v}$ for all $\boldsymbol{v} \in V_h$ and*

$$\left|\Pi_h^1 \boldsymbol{v}_h\right|_{1,\infty,K} \leq C |\boldsymbol{v}_h|_{1,\infty,K} \quad \forall\, K \in \mathcal{T}_h, \boldsymbol{v}_h \in V_h^0, \tag{2.7}$$

$$\left\|\Pi_h^R \boldsymbol{v}_h\right\|_{\infty,K} \leq C h_K |\boldsymbol{v}_h|_{1,\infty,K} \quad \forall\, K \in \mathcal{T}_h, \boldsymbol{v}_h \in V_h^0. \tag{2.8}$$

Finally, we extend the definitions of Π_h, Π_h^1 and Π_h^R to $\operatorname{span}\{\boldsymbol{u}\}$ for the exact solution $\boldsymbol{u}$, by defining that

$$\Pi_h \boldsymbol{u} = \Pi_h^1 \boldsymbol{u} = \boldsymbol{u}, \quad \Pi_h^R \boldsymbol{u} = \boldsymbol{0}. \tag{2.9}$$

Since we have assumed $\boldsymbol{u} \notin V_h$, this extension will not arise contradiction with their definitions on V_h.

In Section 4, we shall show that the reconstruction operators in [37, Remark 4.2] and their higher order versions on a class of locally divergence-free simplicial elements satisfy all the above properties.

2.2. **The EMAPR method for classical elements.** Introduce

$$a(\boldsymbol{u}, \boldsymbol{v}) := (\nabla \boldsymbol{u}, \nabla \boldsymbol{v}) \text{ for all } \boldsymbol{u}, \boldsymbol{v} \in V,$$

and

$$c(\boldsymbol{u}, \boldsymbol{v}, \boldsymbol{w}) := ((\boldsymbol{u} \cdot \nabla)\boldsymbol{v}, \boldsymbol{w}) \text{ for all } (\boldsymbol{u}, \boldsymbol{v}, \boldsymbol{w}) \in \boldsymbol{L}^2(\Omega) \times V \times \boldsymbol{L}^2(\Omega).$$

The weak formulation for (1.1) characterises $(\boldsymbol{u}, p) : J \to V \times W$ by

$$\left(\frac{\partial \boldsymbol{u}}{\partial t}, \boldsymbol{v}\right) + \nu a(\boldsymbol{u}, \boldsymbol{v}) + c(\boldsymbol{u}, \boldsymbol{u}, \boldsymbol{v}) - b(\boldsymbol{v}, p) = (\boldsymbol{f}, \boldsymbol{v}) \quad \forall\ \boldsymbol{v} \in V, \tag{2.10a}$$

$$b(\boldsymbol{u}, q) = 0 \quad \forall\ q \in W, \tag{2.10b}$$

and $\boldsymbol{u}(0) = \boldsymbol{u}^0$. A straightforward semi-discrete analog of (2.10) is to find $(\boldsymbol{u}_h, p_h) : J \to V_h \times W_h$ satisfying $\boldsymbol{u}_h(0) = \boldsymbol{u}_h^0 \in V_h$ with $\boldsymbol{u}_h^0$ some approximation of $\boldsymbol{u}^0$ and

$$\left(\frac{\partial \boldsymbol{u}_h}{\partial t}, \boldsymbol{v}_h\right) + \nu a(\boldsymbol{u}_h, \boldsymbol{v}_h) + c(\boldsymbol{u}_h, \boldsymbol{u}_h, \boldsymbol{v}_h) - b(\boldsymbol{v}_h, p_h) = (\boldsymbol{f}, \boldsymbol{v}_h), \tag{2.11a}$$

$$b(\boldsymbol{u}_h, q_h) = 0, \tag{2.11b}$$

for all $(\boldsymbol{v}_h, q_h) \in V_h \times W_h$. However, it is well-known that the above scheme is not energy-stable and pressure-robust unless $\boldsymbol{u}_h$ is exactly divergence-free (or equivalently, $\nabla \cdot V_h \subseteq W_h$). To obtain a pressure-robust velocity for classical elements, in [37] Linke and Merdon proposed a novel finite element formulation which reads

$$\begin{aligned}\left(\Pi_h \frac{\partial \boldsymbol{u}_h}{\partial t}, \Pi_h \boldsymbol{v}_h\right) + \nu a(\boldsymbol{u}_h, \boldsymbol{v}_h) + c(\boldsymbol{u}_h, \boldsymbol{u}_h, \Pi_h \boldsymbol{v}_h) \\ - b(\boldsymbol{v}_h, p_h) + b(\boldsymbol{u}_h, q_h) = (\boldsymbol{f}, \Pi_h \boldsymbol{v}_h).\end{aligned}$$

Here $b(\boldsymbol{v}_h, p_h)$ should be interpreted as $b(\Pi_h \boldsymbol{v}_h, p_h)$ via property (2.5). By using divergence-free reconstructions, the above formulation restores the L^2-orthogonality between discretely divergence-free test functions and gradient fields, and thus remove the effect of the continuous pressure for velocity errors. There is a consistency error arising from the diffusion term.

To make the method energy-stable, a pressure-robust and energy-conserving discretization (the rotational form) of the nonlinear term were also proposed in [37]:

$$c_{\mathrm{rot}}(\boldsymbol{u}_h, \boldsymbol{v}_h, \boldsymbol{w}_h) := (\nabla \times \boldsymbol{u}_h \times \Pi_h \boldsymbol{v}_h, \Pi_h \boldsymbol{w}_h), \tag{2.12}$$

where $\nabla\times$ is the curl operator [23]. However, following [10] or Section 2.3 below, one can prove that the rotational form does not preserve momentum and angular

momentum (see Remark 4 below). To resolve this issue, we propose an EMA-conserving form, which results in the EMAPR reconstruction:

$$\text{Find } (\boldsymbol{u}_h, p_h) : J \to V_h \times W_h \text{ such that}$$

$$d_h\left(\frac{\partial \boldsymbol{u}_h}{\partial t}, \boldsymbol{v}_h\right) + \nu a\left(\boldsymbol{u}_h, \boldsymbol{v}_h\right) + c_h\left(\boldsymbol{u}_h, \boldsymbol{u}_h, \boldsymbol{v}_h\right) - b\left(\boldsymbol{v}_h, p_h\right) = \left(\boldsymbol{f}, \Pi_h \boldsymbol{v}_h\right), \tag{2.13a}$$

$$b\left(\boldsymbol{u}_h, q_h\right) = 0, \tag{2.13b}$$

for all $\boldsymbol{v}_h \in V_h, q_h \in W_h$ and $\boldsymbol{u}_h(0) = \boldsymbol{u}_h^0$. Here d_h is given by

$$d_h\left(\boldsymbol{u}_h, \boldsymbol{v}_h\right) := \left(\Pi_h \boldsymbol{u}_h, \Pi_h \boldsymbol{v}_h\right) + \alpha\left(\Pi_h^R \boldsymbol{u}_h, \Pi_h^R \boldsymbol{v}_h\right), \tag{2.14}$$

where α is a positive parameter. The trilinear form c_h is defined by

$$\begin{aligned} c_h\left(\boldsymbol{u}_h, \boldsymbol{v}_h, \boldsymbol{w}_h\right) :&= c\left(\Pi_h \boldsymbol{u}_h, \Pi_h^1 \boldsymbol{v}_h, \Pi_h^1 \boldsymbol{w}_h\right) + c\left(\Pi_h \boldsymbol{u}_h, \Pi_h^1 \boldsymbol{v}_h, \Pi_h^R \boldsymbol{w}_h\right) \\ &\quad - c\left(\Pi_h \boldsymbol{u}_h, \Pi_h^1 \boldsymbol{w}_h, \Pi_h^R \boldsymbol{v}_h\right) \\ &= c\left(\Pi_h \boldsymbol{u}_h, \Pi_h^1 \boldsymbol{v}_h, \Pi_h \boldsymbol{w}_h\right) - c\left(\Pi_h \boldsymbol{u}_h, \Pi_h^1 \boldsymbol{w}_h, \Pi_h^R \boldsymbol{v}_h\right). \end{aligned} \tag{2.15}$$

Remark 2. The fundamental requirement of projection Π_h is: For any $\boldsymbol{v}_h \in V_h$, $\Pi_h \boldsymbol{v}_h$ can be decomposed into a sufficiently approximate H^1-conforming component and a "small" $H(\mathrm{div})$-conforming component (consider $\Pi_h^1 \boldsymbol{v}_h$ and $\Pi_h^R \boldsymbol{v}_h$). This is the prerequisite of constructing our methods. Regarding the discretization of the convection term, a rough description of our basic idea is: Apply the H^1-conforming part to guarantee the accuracy and "abuse" the $H(\mathrm{div})$-conforming part to guarantee the conservation of energy, momentum and angular momentum. We note that the reconstruction operators in [34] for Taylor-Hood and MINI elements probably satisfy this fundamental requirement also.

Remark 3. The bilinear form d_h with $\alpha = 0$ is the classical discretization in pressure-robust reconstructions for the $(\boldsymbol{u}, \boldsymbol{v})$-like term. However, for the case $\alpha = 0$ we can not obtain a Re-semi-robust estimate theoretically. In practice, we find that the stabilization term $\left(\Pi_h^R \boldsymbol{u}_h, \Pi_h^R \boldsymbol{v}_h\right)$ is of importance for the high order locally divergence-free elements ($k \geq 2$) in the case that ν is very small or equal to zero (the Euler equation). In this case, without this term, the H^1 error of the discrete velocity might be large.

2.3. **EMA-balance in semi-discrete schemes.** Now we are in the position to analyze the discrete balance laws with the EMAPR reconstruction. We define kinetic energy $E : X \to \mathbb{R}$, momentum $M : X \to \mathbb{R}^d$ and angular momentum $M_{\boldsymbol{x}} : X \to \mathbb{R}^3$ by

$$E\left(\boldsymbol{u}^*\right) := \frac{1}{2}\int_\Omega \left|\boldsymbol{u}^*\right|^2 \, d\boldsymbol{x}, \quad M\left(\boldsymbol{u}^*\right) := \int_\Omega \boldsymbol{u}^* \, d\boldsymbol{x}, \quad M_{\boldsymbol{x}}\left(\boldsymbol{u}^*\right) := \int_\Omega \boldsymbol{u}^* \times \boldsymbol{x} \, d\boldsymbol{x},$$

for any $\boldsymbol{u}^* \in X$. For any two-dimensional vector $\boldsymbol{u}^* = (u_1^*, u_2^*)$, to compute angular momentum or cross product, one can always embed it into three-dimensional spaces by setting $\boldsymbol{u}^* = (u_1^*, u_2^*, 0)$. Let $\boldsymbol{u}$ be the solution of (2.10) and it satisfies the following balance laws [10, 42]:

$$\frac{d}{dt}E\left(\boldsymbol{u}\right) + \nu\left\|\nabla \boldsymbol{u}\right\|^2 = \left(\boldsymbol{f}, \boldsymbol{u}\right), \quad \frac{d}{dt}M\left(\boldsymbol{u}\right) = \int_\Omega \boldsymbol{f} \, d\boldsymbol{x}, \quad \frac{d}{dt}M_{\boldsymbol{x}}\left(\boldsymbol{u}\right) = \int_\Omega \boldsymbol{f} \times \boldsymbol{x} \, d\boldsymbol{x},$$

where the balance laws of momentum and angular momentum are based on some appropriate assumptions. Following [10, 11, 42], here (only for the analysis of

momentum and angular momentum) we assume that $(\boldsymbol{u}, p)$ is compactly supported in Ω (e.g., consider an isolated vortex). We also define a discrete energy $E_d : V_h^0 \oplus \operatorname{span}\{\boldsymbol{u}\} \to \mathbb{R}$ by

$$E_d(\boldsymbol{u}^*) := \frac{1}{2} d_h(\boldsymbol{u}^*, \boldsymbol{u}^*),$$

for any $\boldsymbol{u}^* \in V_h^0 \oplus \operatorname{span}\{\boldsymbol{u}\}$. Note that we have $E(\Pi_h \boldsymbol{u}^*) \le E_d(\boldsymbol{u}^*)$ with $E(\boldsymbol{u}) = E_d(\boldsymbol{u})$.

The following lemma is essential for EMA analysis.

Lemma 1. *For any finite element triple $(\boldsymbol{u}_h, \boldsymbol{v}_h, \boldsymbol{w}_h) \in \boldsymbol{H}(\mathrm{div}; \Omega) \times \boldsymbol{H}^1(\Omega) \times \boldsymbol{H}^1(\Omega)$, we have*

$$c(\boldsymbol{u}_h, \boldsymbol{v}_h, \boldsymbol{w}_h) = -c(\boldsymbol{u}_h, \boldsymbol{w}_h, \boldsymbol{v}_h) \tag{2.16}$$

if

1) *$\boldsymbol{u}_h$ is exactly divergence-free, i.e., $\nabla \cdot \boldsymbol{u}_h \equiv 0$;*
2) *$\boldsymbol{u}_h|_\Gamma \cdot \boldsymbol{n} = 0$ or $\boldsymbol{v}_h|_\Gamma = \boldsymbol{0}$ or $\boldsymbol{w}_h|_\Gamma = \boldsymbol{0}$.*

Proof. This lemma is covered by the lemma for skew-symmetry of a class of discontinuous Galerkin formulations, cf. [17, Lemma 6.39]. In fact, the trilinear form "$t_h(\cdot,\cdot,\cdot)$" in [17, Lemma 6.39] is exactly $c(\cdot,\cdot,\cdot)$ provided that all inputs satisfy the conditions in Lemma 1. Then [17, Lemma 6.39] implies, for $(\boldsymbol{u}_h, \boldsymbol{v}_h, \boldsymbol{w}_h)$ satisfying the conditions in Lemma 1,

$$\begin{aligned} 0 = c(\boldsymbol{u}_h, \boldsymbol{v}_h + \boldsymbol{w}_h, \boldsymbol{v}_h + \boldsymbol{w}_h) = &\underbrace{c(\boldsymbol{u}_h, \boldsymbol{v}_h, \boldsymbol{v}_h)}_{=0} + \underbrace{c(\boldsymbol{u}_h, \boldsymbol{w}_h, \boldsymbol{w}_h)}_{=0} + \\ &c(\boldsymbol{u}_h, \boldsymbol{v}_h, \boldsymbol{w}_h) + c(\boldsymbol{u}_h, \boldsymbol{w}_h, \boldsymbol{v}_h). \end{aligned}$$

This completes the proof. □

Lemma 1 and (2.15) imply the following lemma.

Lemma 2. *For any $(\boldsymbol{u}_h, \boldsymbol{v}_h, \boldsymbol{w}_h) \in V_h^0 \times V_h \times V_h$ we have*

$$c_h(\boldsymbol{u}_h, \boldsymbol{v}_h, \boldsymbol{w}_h) = -c_h(\boldsymbol{u}_h, \boldsymbol{w}_h, \boldsymbol{v}_h).$$

Setting $\boldsymbol{v}_h = \boldsymbol{u}_h$ in (2.13) and applying (2.13b) and Lemma 2, one immediately obtains that

Theorem 2.1. *Let $\boldsymbol{u}_h$ be the solution of (2.13). Then it satisfies the following balance of energy:*

$$\frac{d}{dt} E_d(\boldsymbol{u}_h) + \nu \|\nabla \boldsymbol{u}_h\|^2 = (\boldsymbol{f}, \Pi_h \boldsymbol{u}_h).$$

Boundary conditions may influence the balance of momentum and angular momentum. For simplicity, we do some extra assumptions which are similar to the continuous case, to remove the contribution of boundary. Similar assumptions were also used for the analysis of the EMAC formulation in [10].

Assumption 2. *The finite element solution $(\boldsymbol{u}_h, p_h)$, $\Pi_h \boldsymbol{u}_h$ and the external force $\boldsymbol{f}$ are only supported on a sub-mesh $\hat{\mathcal{T}}_h \subset \mathcal{T}_h$ such that there exists an operator $\chi : \boldsymbol{H}^1(\Omega) \to \boldsymbol{P}^k \subseteq V_h$ satisfying*

$$\chi(\boldsymbol{g})|_{\hat{\mathcal{T}}_h} = \boldsymbol{g}, \quad \Pi_h \chi(\boldsymbol{g})|_{\hat{\mathcal{T}}_h} = \Pi_h^1 \chi(\boldsymbol{g})|_{\hat{\mathcal{T}}_h} = \boldsymbol{g}, \tag{2.18}$$

for $\boldsymbol{g} = \boldsymbol{e}_i, \boldsymbol{x} \times \boldsymbol{e}_i$ $(1 \le i \le d)$. Here $\boldsymbol{e}_i \in \mathbb{R}^d$ is the unit vector whose i-th component is equal to 1.

In fact, for locally divergence-free elements, the support of $\Pi_h \boldsymbol{u}_h$ is the same as $\boldsymbol{u}_h$, since the reconstruction could be locally performed on each element. Furthermore, note that $\nabla \cdot \boldsymbol{e}_i = \nabla \cdot (\boldsymbol{x} \times \boldsymbol{e}_i) = 0$, and $\boldsymbol{e}_i$ and $\boldsymbol{x} \times \boldsymbol{e}_i$ are linear polynomials. So the equalities for Π_h and Π_h^1 in (2.18) are not hard to satisfy. The reconstruction operators in Section 4 fulfill these equalities.

Next, the following equalities will be used to analyze angular momentum:

$$\boldsymbol{a} \cdot (\boldsymbol{b} \times \boldsymbol{c}) = (\boldsymbol{a} \times \boldsymbol{b}) \cdot \boldsymbol{c}, \tag{2.19}$$

and

$$(\boldsymbol{a} \cdot \nabla)(\boldsymbol{x} \times \boldsymbol{e}_i) \cdot \boldsymbol{b} = -(\boldsymbol{a} \times \boldsymbol{b}) \cdot \boldsymbol{e}_i, \tag{2.20}$$

for any $\boldsymbol{a}, \boldsymbol{b}, \boldsymbol{c} \in \mathbb{R}^3$. These two equalities can be obtained by expanding out each term.

Theorem 2.2. *Let $\boldsymbol{u}_h$ be the solution of (2.13). Then under Assumption 2 $\Pi_h u_h$ satisfies the following balances:*

$$\frac{d}{dt} M(\Pi_h \boldsymbol{u}_h) = \int_\Omega \boldsymbol{f} \, d\boldsymbol{x}, \quad \frac{d}{dt} M_{\boldsymbol{x}}(\Pi_h \boldsymbol{u}_h) = \int_\Omega \boldsymbol{f} \times \boldsymbol{x} \, d\boldsymbol{x}.$$

Proof. Taking $\boldsymbol{v}_h = \chi(\boldsymbol{e}_i), \chi(\tilde{\boldsymbol{e}}_i)$ with $\tilde{\boldsymbol{e}}_i := \boldsymbol{x} \times \boldsymbol{e}_i$ in (2.13), by Assumption 2 one respectively obtains

$$\left(\frac{\partial(\Pi_h \boldsymbol{u}_h)}{\partial t}, \boldsymbol{e}_i\right) + \nu a(\boldsymbol{u}_h, \boldsymbol{e}_i) + c_h(\boldsymbol{u}_h, \boldsymbol{u}_h, \boldsymbol{e}_i) - b(\boldsymbol{e}_i, p_h) = (\boldsymbol{f}, \boldsymbol{e}_i),$$

and

$$\left(\frac{\partial(\Pi_h \boldsymbol{u}_h)}{\partial t}, \tilde{\boldsymbol{e}}_i\right) + \nu a(\boldsymbol{u}_h, \tilde{\boldsymbol{e}}_i) + c_h(\boldsymbol{u}_h, \boldsymbol{u}_h, \tilde{\boldsymbol{e}}_i) - b(\tilde{\boldsymbol{e}}_i, p_h) = (\boldsymbol{f}, \tilde{\boldsymbol{e}}_i) = (\boldsymbol{f} \times \boldsymbol{x}, \boldsymbol{e}_i),$$

where in the last inequality we also apply (2.19). Since $\Delta \boldsymbol{e}_i = \Delta \tilde{\boldsymbol{e}}_i = \boldsymbol{0}$ and $\nabla \cdot \boldsymbol{e}_i = \nabla \cdot \tilde{\boldsymbol{e}}_i = 0$, it suffices to prove that

$$c_h(\boldsymbol{u}_h, \boldsymbol{u}_h, \boldsymbol{e}_i) = 0, \quad c_h(\boldsymbol{u}_h, \boldsymbol{u}_h, \tilde{\boldsymbol{e}}_i) = 0.$$

By $\nabla \boldsymbol{e}_i = \boldsymbol{0}$, Lemma 2 and (2.18) imply that

$$c_h(\boldsymbol{u}_h, \boldsymbol{u}_h, \boldsymbol{e}_i) = -c_h(\boldsymbol{u}_h, \boldsymbol{e}_i, \boldsymbol{u}_h) = -c(\Pi_h \boldsymbol{u}_h, \boldsymbol{e}_i, \Pi_h \boldsymbol{u}_h) = 0,$$

and

$$c_h(\boldsymbol{u}_h, \boldsymbol{u}_h, \tilde{\boldsymbol{e}}_i) = -c(\Pi_h \boldsymbol{u}_h, \tilde{\boldsymbol{e}}_i, \Pi_h \boldsymbol{u}_h) = (\Pi_h \boldsymbol{u}_h \times \Pi_h \boldsymbol{u}_h, \boldsymbol{e}_i) = 0,$$

together with (2.20). Thus we complete the proof. □

For the case $\nu = 0$ (the Euler equations), if we apply the no-penetration boundary condition ($\boldsymbol{u} \cdot \boldsymbol{n} = 0$ on $J \times \Gamma$), the skew-symmetry of c_h still holds by Lemma 1. Thus Theorem 2.1 implies that the method (2.13) conserves a discrete energy for $\nu = 0$ and $\boldsymbol{f} = \boldsymbol{0}$, with only no-penetration boundary condition strongly imposed. Theorem 2.2 implies that (2.13) conserves linear momentum and angular momentum (of $\Pi_h \boldsymbol{u}_h$) for $\boldsymbol{f}$ with zero momentum and zero angular momentum, respectively (under Assumption 2).

Remark 4 (Momentum analysis for the rotational form (2.12)). We use linear momentum as an example. By [10, Eq. (8)], we have

$$c_{\mathrm{rot}}(\boldsymbol{u}_h, \boldsymbol{u}_h, \boldsymbol{v}_h) = c(\Pi_h \boldsymbol{u}_h, \boldsymbol{u}_h, \Pi_h \boldsymbol{v}_h) - c(\Pi_h \boldsymbol{v}_h, \boldsymbol{u}_h, \Pi_h \boldsymbol{u}_h).$$

Then taking $\boldsymbol{v}_h = \chi(\boldsymbol{e}_i)$ gives

$$\begin{aligned} c_{\text{rot}}(\boldsymbol{u}_h, \boldsymbol{u}_h, \boldsymbol{e}_i) &= c(\Pi_h \boldsymbol{u}_h, \boldsymbol{u}_h, \boldsymbol{e}_i) - c(\boldsymbol{e}_i, \boldsymbol{u}_h, \Pi_h \boldsymbol{u}_h) \\ &= -c(\Pi_h \boldsymbol{u}_h, \boldsymbol{e}_i, \boldsymbol{u}_h) - c(\boldsymbol{e}_i, \boldsymbol{u}_h, \Pi_h \boldsymbol{u}_h) \quad \text{(by Lemma 1)} \\ &= -c(\boldsymbol{e}_i, \boldsymbol{u}_h, \Pi_h \boldsymbol{u}_h) \neq 0. \end{aligned}$$

Thus linear momentum is not preserved by c_{rot}. Angular momentum can be similarly checked.

3. A pressure-robust and Re-semi-robust error estimate

Let $\boldsymbol{u}$ solve (2.10). We assume $\Delta \boldsymbol{u} \in L^2\left(J; \boldsymbol{L}^2(\Omega)\right)$. Multiplying $\Pi_h \boldsymbol{v}_h \in \Pi_h V_h^0$ on the two sides of (1.1) and integrating over Ω, one arrives at

$$\left(\frac{\partial \boldsymbol{u}}{\partial t}, \Pi_h \boldsymbol{v}_h\right) - \nu(\Delta \boldsymbol{u}, \Pi_h \boldsymbol{v}_h) + c(\boldsymbol{u}, \boldsymbol{u}, \Pi_h \boldsymbol{v}_h) = (\boldsymbol{f}, \Pi_h \boldsymbol{v}_h) \quad \forall\ \boldsymbol{v}_h \in V_h^0, \tag{3.1}$$

where the term $(\nabla p, \Pi_h \boldsymbol{v}_h)$ has been removed since $\nabla \cdot \Pi_h \boldsymbol{v}_h \equiv 0$. According to the definition of Π_h, Π_h^1 and Π_h^R on the exact solution $\boldsymbol{u}$ (see Eq. (2.9)) and (2.14) and (2.15), Eq. (3.1) could be rewritten as

$$d_h\left(\frac{\partial \boldsymbol{u}}{\partial t}, \boldsymbol{v}_h\right) - \nu(\Delta \boldsymbol{u}, \Pi_h \boldsymbol{v}_h) + c_h(\boldsymbol{u}, \boldsymbol{u}, \boldsymbol{v}_h) = (\boldsymbol{f}, \Pi_h \boldsymbol{v}_h) \quad \forall\ \boldsymbol{v}_h \in V_h^0. \tag{3.2}$$

Subtracting (2.13) from (3.1) we get the error equation

$$\begin{aligned} d_h\left(\frac{\partial(\boldsymbol{u} - \boldsymbol{u}_h)}{\partial t}, \boldsymbol{v}_h\right) &+ \nu(\nabla(\boldsymbol{u} - \boldsymbol{u}_h), \nabla \boldsymbol{v}_h) + c_h(\boldsymbol{u}, \boldsymbol{u}, \boldsymbol{v}_h) \\ &- c_h(\boldsymbol{u}_h, \boldsymbol{u}_h, \boldsymbol{v}_h) = \delta_h(\boldsymbol{u}, \boldsymbol{v}_h) \quad \forall\ \boldsymbol{v}_h \in V_h^0, \end{aligned} \tag{3.3}$$

where

$$\delta_h(\boldsymbol{u}, \boldsymbol{v}_h) := \nu(\Delta \boldsymbol{u}, \Pi_h \boldsymbol{v}_h) + \nu(\nabla \boldsymbol{u}, \nabla \boldsymbol{v}_h) = -\nu(\Delta \boldsymbol{u}, (1 - \Pi_h)\boldsymbol{v}_h)$$

is the consistency error from the diffusion term [36, 37].

Denote by $\Pi_h^S : V^0 \to V_h^0$ the Stokes projection which satisfies

$$\left(\nabla\left(\boldsymbol{v} - \Pi_h^S \boldsymbol{v}\right), \nabla \boldsymbol{w}\right) = 0 \quad \forall\ \boldsymbol{v} \in V^0, \boldsymbol{w} \in V_h^0. \tag{3.4}$$

Assumption 3. *For any $\boldsymbol{v} \in V^0 \cap \boldsymbol{W}^{1,\infty}(\Omega)$, it holds that*

$$\left\|\nabla \Pi_h^S \boldsymbol{v}\right\|_\infty \leq C \|\nabla \boldsymbol{v}\|_\infty. \tag{3.5}$$

We refer the readers to [22] for some analysis of (3.5).

Split the error $\boldsymbol{u} - \boldsymbol{u}_h$ as

$$\boldsymbol{e}_h := \boldsymbol{u} - \boldsymbol{u}_h = \boldsymbol{u} - \Pi_h^S \boldsymbol{u} + \Pi_h^S \boldsymbol{u} - \boldsymbol{u}_h = \boldsymbol{\eta} + \boldsymbol{\phi}_h. \tag{3.6}$$

Next, we introduce the dual norm $\|\cdot\|_{(V_h^0)'}$ for any linear functional L on V_h^0:

$$\|L\|_{\left(V_h^0\right)'} := \sup_{\boldsymbol{v}_h \in V_h^0 \setminus \{\boldsymbol{0}\}} \frac{L(\boldsymbol{v}_h)}{\|\nabla \boldsymbol{v}_h\|},$$

or for any $\boldsymbol{g} \in \boldsymbol{L}^2(\Omega)$:

$$\|\boldsymbol{g}\|_{\left(V_h^0\right)'} := \sup_{\boldsymbol{v}_h \in V_h^0 \setminus \{\boldsymbol{0}\}} \frac{(\boldsymbol{g}, \boldsymbol{v}_h)}{\|\nabla \boldsymbol{v}_h\|}.$$

We also define a mesh-dependent seminorm $|||\cdot|||_*$ on V_h by

$$|||\boldsymbol{w}|||_*^2 := \sum_{K\in\mathcal{T}_h} h_K^{-2} \left\|\Pi_h^R \boldsymbol{w}\right\|_K^2. \tag{3.7}$$

The following two inequalities will be used to estimate the nonlinear terms.

Lemma 3. *There exists a positive constant C, independent of h, such that*

$$c\left(\boldsymbol{z},\boldsymbol{v},\Pi_h^R\boldsymbol{w}\right) \le C\left\|\boldsymbol{z}\right\|_\infty \left\|\boldsymbol{v}\right\| |||\boldsymbol{w}|||_*, \tag{3.8}$$

and

$$c\left(\boldsymbol{z},\boldsymbol{v},\Pi_h^R\boldsymbol{w}\right) \le C\left\|\boldsymbol{z}\right\| \left\|\boldsymbol{v}\right\| |\boldsymbol{w}|_{1,\infty}, \tag{3.9}$$

for $(\boldsymbol{z},\boldsymbol{v},\boldsymbol{w}) \in \boldsymbol{L}^2(\Omega)\times V_h \times V_h^0$ with some corresponding regularity conditions.

Proof. It follows from the Schwarz's inequality and the inverse inequality that

$$\begin{aligned} c\left(\boldsymbol{z},\boldsymbol{v},\Pi_h^R\boldsymbol{w}\right) &= \sum_{K\in\mathcal{T}_h} \left((\boldsymbol{z}\cdot\nabla)\boldsymbol{v},\Pi_h^R\boldsymbol{w}\right)_K \le \left\|\boldsymbol{z}\right\|_\infty \sum_{K\in\mathcal{T}_h} \left\|\nabla\boldsymbol{v}\right\|_K \left\|\Pi_h^R\boldsymbol{w}\right\|_K \\ &\le \left\|\boldsymbol{z}\right\|_\infty \left(\sum_{K\in\mathcal{T}_h} h_K^2 \left\|\nabla\boldsymbol{v}\right\|_K^2\right)^{1/2} \left(\sum_{K\in\mathcal{T}_h} h_K^{-2}\left\|\Pi_h^R\boldsymbol{w}\right\|_K^2\right)^{1/2} \\ &\le C\left\|\boldsymbol{z}\right\|_\infty \left\|\boldsymbol{v}\right\| |||\boldsymbol{w}|||_*. \end{aligned}$$

For the second inequality, from (2.8) similarly we have

$$\begin{aligned} c\left(\boldsymbol{z},\boldsymbol{v},\Pi_h^R\boldsymbol{w}\right) &= \sum_{K\in\mathcal{T}_h} \left((\boldsymbol{z}\cdot\nabla)\boldsymbol{v},\Pi_h^R\boldsymbol{w}\right)_K \le \sum_{K\in\mathcal{T}_h} \left\|\boldsymbol{z}\right\|_K \left\|\nabla\boldsymbol{v}\right\|_K \left\|\Pi_h^R\boldsymbol{w}\right\|_{\infty,K} \\ &\le \sum_{K\in\mathcal{T}_h} \left\|\boldsymbol{z}\right\|_K h_K \left\|\nabla\boldsymbol{v}\right\|_K h_K^{-1} \left\|\Pi_h^R\boldsymbol{w}\right\|_{\infty,K} \\ &\le C\sum_{K\in\mathcal{T}_h} \left\|\boldsymbol{z}\right\|_K \left\|\boldsymbol{v}\right\|_K |\boldsymbol{w}|_{1,\infty,K} \le C\left\|\boldsymbol{z}\right\| \left\|\boldsymbol{v}\right\| |\boldsymbol{w}|_{1,\infty}. \end{aligned}$$

This completes the proof. □

Theorem 3.1. *Let $\boldsymbol{u}$ be the solution of (2.10) and $\boldsymbol{u}_h$ be the solution of (2.13). Under Assumption 1, Assumption 3 and the assumptions that $\boldsymbol{u}\in L^2\left(J;\boldsymbol{W}^{1,\infty}(\Omega)\right)\cap L^4\left(J;\boldsymbol{H}^1(\Omega)\right)$, $\boldsymbol{u}_t\in L^2\left(J;\boldsymbol{L}^2(\Omega)\right)$, $\Delta\boldsymbol{u}\in L^2\left(J;\boldsymbol{L}^2(\Omega)\right)$ and $\boldsymbol{u}_h^0 = \Pi_h^S\boldsymbol{u}^0$, with C independent of h and ν the following estimate holds:*

$$\begin{aligned} E_d(\boldsymbol{e}_h(T)) + \frac{\nu}{2}\int_0^T \left\|\nabla\boldsymbol{e}_h\right\|^2 \,dt &\le E_d(\boldsymbol{\eta}(T)) + \frac{\nu}{2}\int_0^T \left\|\nabla\boldsymbol{\eta}\right\|^2 \,dt \\ &+ e^{G(\boldsymbol{u},T)}\int_0^T \left\{ E_d(\boldsymbol{\eta}_t) + \frac{\nu}{2}\left\|\Delta\boldsymbol{u}\circ(1-\Pi_h)\right\|_{(V_h^0)'}^2 \right. \\ &\left. + C\left\|\boldsymbol{u}\right\|_{1,\infty}\left(\left\|\Pi_h\boldsymbol{\eta}\right\|^2 + \left\|\nabla\Pi_h^1\boldsymbol{\eta}\right\|^2 + |||\boldsymbol{\eta}|||_*^2\right)\right\} dt, \end{aligned} \tag{3.10}$$

where $G(\boldsymbol{u},T) = T + C_\alpha\left\|\boldsymbol{u}\right\|_{L^1(J;\boldsymbol{W}^{1,\infty}(\Omega))}$ with C_α dependent on α and the shape regularity of mesh but independent of h and ν.

Proof. Substituting (3.6) into (3.3) and taking $\boldsymbol{v}_h = \boldsymbol{\phi}_h$ give that

$$\begin{aligned}\frac{d}{dt}E_d\left(\boldsymbol{\phi}_h\right) + \nu\left\|\nabla\boldsymbol{\phi}_h\right\|^2 = d_h\left(\boldsymbol{\eta}_t, \boldsymbol{\phi}_h\right) - \underbrace{\nu\left(\nabla\boldsymbol{\eta}, \nabla\boldsymbol{\phi}_h\right)}_{=0 \text{ by } (3.4)} \\ \underbrace{-c_h\left(\boldsymbol{u}, \boldsymbol{u}, \boldsymbol{\phi}_h\right) + c_h\left(\boldsymbol{u}_h, \boldsymbol{u}_h, \boldsymbol{\phi}_h\right)}_{\mathcal{NL}} + \delta_h\left(\boldsymbol{u}, \boldsymbol{\phi}_h\right).\end{aligned} \tag{3.11}$$

Let us estimate each term in (3.11). For the evolutionary term we have

$$\left|d_h\left(\boldsymbol{\eta}_t, \boldsymbol{\phi}_h\right)\right| \leq E_d\left(\boldsymbol{\eta}_t\right) + E_d\left(\boldsymbol{\phi}_h\right). \tag{3.12}$$

For δ_h the estimate could be found in [37]:

$$\left|\delta_h\left(\boldsymbol{u}, \boldsymbol{\phi}_h\right)\right| \leq \frac{1}{2}\nu\left\|\Delta\boldsymbol{u} \circ \left(1 - \Pi_h\right)\right\|^2_{\left(V_h^0\right)'} + \frac{1}{2}\nu\left\|\nabla\boldsymbol{\phi}_h\right\|^2. \tag{3.13}$$

Now, let us estimate the convective terms. We use a similar decomposition with [42, 46]:

$$-\mathcal{NL} = c_h\left(\boldsymbol{u}, \boldsymbol{\eta}, \boldsymbol{\phi}_h\right) + c_h\left(\boldsymbol{u}, \Pi_h^S\boldsymbol{u}, \boldsymbol{\phi}_h\right) - c_h\left(\boldsymbol{u}_h, \boldsymbol{u}_h, \boldsymbol{\phi}_h\right). \tag{3.14}$$

Further,

$$\begin{aligned}c_h\left(\boldsymbol{u}, \Pi_h^S\boldsymbol{u}, \boldsymbol{\phi}_h\right) - c_h\left(\boldsymbol{u}_h, \boldsymbol{u}_h, \boldsymbol{\phi}_h\right) &= c_h\left(\boldsymbol{e}_h, \Pi_h^S\boldsymbol{u}, \boldsymbol{\phi}_h\right) + c_h\left(\boldsymbol{u}_h, \Pi_h^S\boldsymbol{u}, \boldsymbol{\phi}_h\right) \\ &\quad - c_h\left(\boldsymbol{u}_h, \boldsymbol{u}_h, \boldsymbol{\phi}_h\right) \\ &= c_h\left(\boldsymbol{e}_h, \Pi_h^S\boldsymbol{u}, \boldsymbol{\phi}_h\right) + c_h\left(\boldsymbol{u}_h, \boldsymbol{\phi}_h, \boldsymbol{\phi}_h\right) \\ &= c_h\left(\boldsymbol{e}_h, \Pi_h^S\boldsymbol{u}, \boldsymbol{\phi}_h\right) \\ &= c_h\left(\boldsymbol{\eta}, \Pi_h^S\boldsymbol{u}, \boldsymbol{\phi}_h\right) + c_h\left(\boldsymbol{\phi}_h, \Pi_h^S\boldsymbol{u}, \boldsymbol{\phi}_h\right).\end{aligned} \tag{3.15}$$

Then it follows from the Schwarz's inequality, Young's inequality, Lemma 3, Assumption 1 and Assumption 3 that

$$\begin{aligned}\left|c_h(\boldsymbol{u},\boldsymbol{\eta}, \boldsymbol{\phi}_h)\right| &= \left|c\left(\boldsymbol{u}, \Pi_h^1\boldsymbol{\eta}, \Pi_h\boldsymbol{\phi}_h\right) - c\left(\boldsymbol{u}, \Pi_h^1\boldsymbol{\phi}_h, \Pi_h^R\boldsymbol{\eta}\right)\right|_{\left(\Pi_h^R\boldsymbol{\eta} = -\Pi_h^R\Pi_h^S\boldsymbol{u}\right)} \\ &\leq \|\boldsymbol{u}\|_\infty\left(\left\|\nabla\Pi_h^1\boldsymbol{\eta}\right\|\left\|\Pi_h\boldsymbol{\phi}_h\right\| + C\left\|\Pi_h^1\boldsymbol{\phi}_h\right\|\left|||\Pi_h^S\boldsymbol{u}|||_*\right)\right. \\ &\leq \|\boldsymbol{u}\|_\infty\left(\frac{1}{2}\left\|\nabla\Pi_h^1\boldsymbol{\eta}\right\|^2 + \frac{1}{2}\left\|\Pi_h\boldsymbol{\phi}_h\right\|^2 + C\left(\left\|\Pi_h^1\boldsymbol{\phi}_h\right\|^2 + |||\boldsymbol{\eta}|||_*^2\right)\right),\end{aligned} \tag{3.16}$$

$$\begin{aligned}\left|c_h\left(\boldsymbol{\eta}, \Pi_h^S\boldsymbol{u}, \boldsymbol{\phi}_h\right)\right| &= \left|c\left(\Pi_h\boldsymbol{\eta}, \Pi_h^1\Pi_h^S\boldsymbol{u}, \Pi_h\boldsymbol{\phi}_h\right) - c\left(\Pi_h\boldsymbol{\eta}, \Pi_h^1\boldsymbol{\phi}_h, \Pi_h^R\Pi_h^S\boldsymbol{u}\right)\right| \\ &\leq C\left|\boldsymbol{u}\right|_{1,\infty}\left\|\Pi_h\boldsymbol{\eta}\right\|\left(\left\|\Pi_h\boldsymbol{\phi}_h\right\| + \left\|\Pi_h^1\boldsymbol{\phi}_h\right\|\right) \\ &\leq C\left|\boldsymbol{u}\right|_{1,\infty}\left(\left\|\Pi_h\boldsymbol{\eta}\right\|^2 + \left\|\Pi_h\boldsymbol{\phi}_h\right\|^2 + \left\|\Pi_h^1\boldsymbol{\phi}_h\right\|^2\right),\end{aligned} \tag{3.17}$$

and

$$\begin{aligned}\left|c_h\left(\boldsymbol{\phi}_h, \Pi_h^S\boldsymbol{u}, \boldsymbol{\phi}_h\right)\right| &= \left|c\left(\Pi_h\boldsymbol{\phi}_h, \Pi_h^1\Pi_h^S\boldsymbol{u}, \Pi_h\boldsymbol{\phi}_h\right)\right. \\ &\left. - c\left(\Pi_h\boldsymbol{\phi}_h, \Pi_h^1\boldsymbol{\phi}_h, \Pi_h^R\Pi_h^S\boldsymbol{u}\right)\right| \leq C\left|\boldsymbol{u}\right|_{1,\infty}\left(\left\|\Pi_h\boldsymbol{\phi}_h\right\|^2 + \left\|\Pi_h^1\boldsymbol{\phi}_h\right\|^2\right).\end{aligned} \tag{3.18}$$

Substituting (3.15)-(3.18) into (3.14) one could obtain that

$$\left|\mathcal{NL}\right| \leq C\left\|\boldsymbol{u}\right\|_{1,\infty}\left(\left\|\Pi_h\boldsymbol{\eta}\right\|^2 + \left\|\nabla\Pi_h^1\boldsymbol{\eta}\right\|^2 + |||\boldsymbol{\eta}|||_*^2 + \left\|\Pi_h\boldsymbol{\phi}_h\right\|^2 + \left\|\Pi_h^1\boldsymbol{\phi}_h\right\|^2\right). \tag{3.19}$$

TABLE 1. Local velocity spaces on an element K.

Order	Dimension	Local space
$k=1$	2D/3D	$\boldsymbol{\mathcal{P}}_k(K)=\left[P^1(K)\right]^d\oplus\operatorname{span}\{\boldsymbol{b}_i,1\le i\le d+1\}$
$k\ge 2$	2D	$\boldsymbol{\mathcal{P}}_k(K)=\left[P^k(K)\oplus b_K\tilde{P}^{k-2}(K)\right]^2$
$k=2$	3D	$\boldsymbol{\mathcal{P}}_k(K)=\left[P^2(K)\oplus b_K\tilde{P}^0(K)\right]^3\oplus\operatorname{span}\{\boldsymbol{b}_i,1\le i\le 4\}$
$k\ge 3$	3D	$\boldsymbol{\mathcal{P}}_k(K)=\left[P^k(K)\oplus b_K\left(\tilde{P}^{k-2}(K)\oplus\tilde{P}^{k-3}(K)\right)\right]^3$

Then substituting (3.12), (3.13) and (3.19) into (3.11) provides

$$\begin{aligned}\frac{d}{dt}E_d(\boldsymbol{\phi}_h)+\frac{\nu}{2}\|\nabla\boldsymbol{\phi}_h\|^2 &\le E_d(\boldsymbol{\eta}_t)+E_d(\boldsymbol{\phi}_h)+\frac{1}{2}\nu\|\Delta\boldsymbol{u}\circ(1-\Pi_h)\|^2_{(V_h^0)'}\\ &+C\|\boldsymbol{u}\|_{1,\infty}\left(\|\Pi_h\boldsymbol{\eta}\|^2+\left\|\nabla\Pi_h^1\boldsymbol{\eta}\right\|^2+|||\boldsymbol{\eta}|||_*^2+\|\Pi_h\boldsymbol{\phi}_h\|^2+\left\|\Pi_h^1\boldsymbol{\phi}_h\right\|^2\right).\end{aligned}\tag{3.20}$$

Note that $\|\Pi_h\boldsymbol{\phi}_h\|^2\le 2E_d(\boldsymbol{\phi}_h)$ and $\left\|\Pi_h^1\boldsymbol{\phi}_h\right\|^2\le(4+4/\alpha)E_d(\boldsymbol{\phi}_h)$ by [7, Lemma 3]. Finally, integrating over J, and applying the fact $\boldsymbol{u}_h(0)=\Pi_h^S\boldsymbol{u}(0)$ and the Gronwall inequality, we can get

$$\begin{aligned}E_d(\boldsymbol{\phi}_h(T))+\frac{\nu}{2}\int_0^T\|\nabla\boldsymbol{\phi}_h\|^2\,dt &\le e^{G(\boldsymbol{u},T)}\int_0^T\left\{E_d(\boldsymbol{\eta}_t)+\frac{\nu}{2}\|\Delta\boldsymbol{u}\circ(1-\Pi_h)\|^2_{(V_h^0)'}\right.\\ &\left.+C\|\boldsymbol{u}\|_{1,\infty}\left(\|\Pi_h\boldsymbol{\eta}\|^2+\left\|\nabla\Pi_h^1\boldsymbol{\eta}\right\|^2+|||\boldsymbol{\eta}|||_*^2\right)\right\}dt.\end{aligned}$$

Then (3.10) follows immediately from a combination of the above inequality and the triangle inequality. □

4. The reconstruction on simiplicial locally mass-conserving elements

In this section, we focus on a class of simiplicial locally divergence-free elements which satisfy the inf-sup condition (2.2), and give the corresponding divergence-free reconstruction operators. First, let us recall the construction of the locally divergence-free elements in [23, pp. 132-144], where the lowest order case is the well-known Bernardi-Raugel element [4]. Consider an arbitrary element K with vertices $a_i, 1\le i\le d+1$. Denote by e_i the edge/face opposite to a_i and $\boldsymbol{n}_i$ the unit outward normal vector corresponding to $e_i, 1\le i\le d+1$. Further, $\lambda_i, 1\le i\le d+1$ denote the corresponding barycentric coordinates. Then the face bubbles are defined by

$$\boldsymbol{b}_i:=\left(\prod_{1\le j\le d+1;j\ne i}\lambda_j\right)\boldsymbol{n}_i, 1\le i\le d+1.$$

We also define

$$b_K:=\prod_{1\le j\le d+1}\lambda_j,\quad \tilde{P}^k(K):=\operatorname{span}\left\{\prod_{i=1}^d x_i^{k_i}, k_i\ge 0, 1\le i\le d, \sum_{i=1}^d k_i=k\right\}.$$

Then the local finite element spaces for velocity on an element K are defined as Table 1. For k-th order velocity spaces, the matching pressure space is the space

of discontinuous piecewise polynomials of degree no more than $k-1$, whatever the dimension is. In what follows, V_h will denote a velocity space of order k mentioned above and W_h is the corresponding pressure space. From Table 1 one can see there exists a space of bubble functions $V_h^b \cong V_h/\boldsymbol{P}^k$ such that $V_h = \boldsymbol{P}^k \oplus V_h^b$. For any $\boldsymbol{v}_h \in V_h$, it is natural to split it into two parts:

$$\boldsymbol{v}_h = \boldsymbol{v}_h^1 + \boldsymbol{v}_h^b \text{ with } \boldsymbol{v}_h^1 \in \boldsymbol{P}^k, \boldsymbol{v}_h^b \in V_h^b.$$

We consider a class of divergence-free reconstruction operators which were also discussed in [37, Remark 4.2]. These operators are defined as follows. Let $I_h : \boldsymbol{C}^0\left(\bar{\Omega}\right) \to \boldsymbol{P}^k$ denote the usual nodal interpolation operator. Then Π_h^1 is defined by

$$\Pi_h^1|_{V_h} := I_h.$$

Let Π_h^{RT} be the common Raviart-Thomas interpolation of order $k-1$ [5]. The operator Π_h^R is defined by

$$\Pi_h^R|_{V_h} := \Pi_h^{RT} \circ (1 - I_h). \tag{4.1}$$

Hence, for any $\boldsymbol{v}_h \in V_h$ one has

$$\Pi_h \boldsymbol{v}_h = \Pi_h^1 \boldsymbol{v}_h + \Pi_h^R \boldsymbol{v}_h = I_h \boldsymbol{v}_h + \Pi_h^{RT}\left(\boldsymbol{v}_h - I_h \boldsymbol{v}_h\right). \tag{4.2}$$

At this time the space X_h could be chosen as

$$X_h := \left\{ \boldsymbol{v}_h \in \boldsymbol{H}\left(\mathrm{div}; \Omega\right) : \boldsymbol{v}_h|_K \in \left[P^k\left(K\right)\right]^d \text{ for all } K \in \mathcal{T}_h \right\}.$$

Clearly X_h and W_h satisfy the relationship (2.3).

Remark 5. Under the setting above, for any $\boldsymbol{v}_h \in V_h$ it holds that $\Pi_h \boldsymbol{v}_h = \boldsymbol{v}_h^1 + \Pi_h \boldsymbol{v}_h^b$. In other words, these reconstruction operators only change the bubble part of the elements. Thus the reconstruction is low-cost and has not changed much compared to the previous classical formulation. This is especially the case for the first order element and the second order element in two dimensions, and the first order element in three dimensions, since it is not hard to find that, for any $\boldsymbol{v}_h$ belonging to these spaces,

$$\Pi_h^1 \boldsymbol{v}_h^b = 0 \Rightarrow \Pi_h \boldsymbol{v}_h^b = \Pi_h^R \boldsymbol{v}_h^b = \Pi_h^{RT} \boldsymbol{v}_h^b \Rightarrow \Pi_h \boldsymbol{v}_h = \boldsymbol{v}_h^1 + \Pi_h^{RT} \boldsymbol{v}_h^b.$$

Next, let us analyze the properties of the reconstruction operators defined above. To analyze the convergence rates of EMAPR for the elements mentioned above, we shall assume that the true solution $\boldsymbol{u}(t)$ $(t \in J)$ is in $\boldsymbol{H}^{\frac{3}{2}+\epsilon}(\Omega)$ with some $\epsilon > 0$. This assumption guarantees $\boldsymbol{u}(t) \in \boldsymbol{C}^0\left(\bar{\Omega}\right)$ and thus $I_h \boldsymbol{u}$ is well-defined. We define $\boldsymbol{V}\left(\mathcal{T}_h\right) := \boldsymbol{C}^0\left(\bar{\Omega}\right) \cap \boldsymbol{H}^2\left(\mathcal{T}_h\right)$.

Lemma 4. *The operators I_h and Π_h^{RT} satisfy the following properties:*

$$\|\boldsymbol{v} - I_h \boldsymbol{v}\|_K + h_K \|\nabla(\boldsymbol{v} - I_h \boldsymbol{v})\|_K \le C h_K^2 |\boldsymbol{v}|_{2,K} \quad \forall\ \boldsymbol{v} \in \boldsymbol{V}\left(\mathcal{T}_h\right); \tag{4.3}$$

$$\|\boldsymbol{v} - I_h \boldsymbol{v}\|_K + h_K \|\nabla(\boldsymbol{v} - I_h \boldsymbol{v})\|_K \le C h_K^2 |\boldsymbol{v} - I_h \boldsymbol{v}|_{2,K} \quad \forall\ \boldsymbol{v} \in \boldsymbol{V}\left(\mathcal{T}_h\right); \tag{4.4}$$

$$\left\|\boldsymbol{v} - \Pi_h^{RT} \boldsymbol{v}\right\|_K \le C h_K \|\nabla \boldsymbol{v}\|_K \quad \forall\ \boldsymbol{v} \in V; \tag{4.5}$$

$$\left\|\Pi_h^{RT} \boldsymbol{v}_h\right\|_{p,K} \le \|\boldsymbol{v}_h\|_{p,K}, \quad p = 2, \infty, \quad \forall\ \boldsymbol{v}_h \in V_h; \tag{4.6}$$

$$\left(\boldsymbol{v} - \Pi_h^{RT} \boldsymbol{v}, \boldsymbol{w}\right)_K = 0 \quad \forall\ \boldsymbol{v} \in V, \boldsymbol{w} \in \left[P^{k-2}(K)\right]^d, \tag{4.7}$$

for all $K \in \mathcal{T}_h$.

Proof. We refer the readers to [6, Theorem 4.4.4] and [5, Propositions 2.5.1, 2.3.4] for (4.3), (4.5) and (4.7), respectively. Note that $I_h(\boldsymbol{v} - I_h\boldsymbol{v}) = \mathbf{0}$. Then replacing $\boldsymbol{v}$ with $\boldsymbol{v} - I_h\boldsymbol{v}$ in (4.3) gives (4.4).

Let us prove (4.6). We have

$$\begin{aligned}\left\|\boldsymbol{v}_h - \Pi_h^{RT}\boldsymbol{v}_h\right\|_{p,K} &\le Ch_K^{d/p-d/2}\left\|\boldsymbol{v}_h - \Pi_h^{RT}\boldsymbol{v}_h\right\|_K \\ &\le Ch_K^{d/p-d/2+1}\left\|\nabla\boldsymbol{v}_h\right\|_K \le C\left\|\boldsymbol{v}_h\right\|_{p,K},\end{aligned}$$

where we repeatedly use the local estimates in [6, Lemma 4.5.3] and the interpolation error of Π_h^{RT} (4.5). Then (4.6) follows immediately from the triangle inequality. Note that (4.6) does not hold if $\boldsymbol{v}_h$ is an arbitrary function in V. □

Lemma 5. *The reconstruction operators defined by (4.2) satisfy (2.4)-(2.8) and (2.18).*

Proof. Eq. (2.18) is clearly satisfied. Furthermore since (2.4) is implied in (2.5) due to $\nabla\cdot\Pi_h\boldsymbol{v}_h \in W_h$ for any $\boldsymbol{v}_h \in V_h$ (see (2.3)), we only prove (2.5)-(2.8).

Denote by $P_h : L^2(\Omega) \to W_h$ the L^2 projection to W_h. Applying the commuting diagram property for Π_h^{RT} and P_h (e.g., see [5, Remark 2.5.2]) and (2.3) one can obtain

$$\begin{aligned}P_h\nabla\cdot\Pi_h\boldsymbol{v}_h = \nabla\cdot\Pi_h\boldsymbol{v}_h &= \nabla\cdot\Pi_h^1\boldsymbol{v}_h + \nabla\cdot\Pi_h^{RT}\left(1-\Pi_h^1\right)\boldsymbol{v}_h \\ &= \nabla\cdot\Pi_h^1\boldsymbol{v}_h + P_h\nabla\cdot\left(1-\Pi_h^1\right)\boldsymbol{v}_h = P_h\nabla\cdot\boldsymbol{v}_h,\end{aligned}$$

which is exactly (2.5).

The proof of (2.6) is very similar to the analysis in [36]. In fact, for any $\boldsymbol{v}_h \in V_h$, from (4.2) we have

$$\boldsymbol{v}_h - \Pi_h\boldsymbol{v}_h = (\boldsymbol{v}_h - I_h\boldsymbol{v}_h) - \Pi_h^{RT}(\boldsymbol{v}_h - I_h\boldsymbol{v}_h), \tag{4.8}$$

which, together with (4.7), implies that

$$(\boldsymbol{v}_h - \Pi_h\boldsymbol{v}_h, \boldsymbol{w})_K = 0 \quad \forall\ \boldsymbol{w} \in \left[P^{k-2}(K)\right]^d, K \in \mathcal{T}_h. \tag{4.9}$$

On the other hand, from (4.8), (4.6), (4.3) and inverse inequalities, it follows that

$$\left\|\boldsymbol{v}_h - \Pi_h\boldsymbol{v}_h\right\|_K \le C\left\|(1-I_h)\boldsymbol{v}_h\right\|_K \le Ch_K^2\left|\boldsymbol{v}_h\right|_{2,K} \le Ch_K\left\|\nabla\boldsymbol{v}_h\right\|_K. \tag{4.10}$$

Then a combination of (4.9), (4.10) and approximation theory gives

$$\left|(\boldsymbol{g}, (1-\Pi_h)\boldsymbol{v}_h)\right| = \left|\left(\boldsymbol{g} - P_h^{k-2}\boldsymbol{g}, (1-\Pi_h)\boldsymbol{v}_h\right)\right| \le Ch^k\left|\boldsymbol{g}\right|_{k-1}\left\|\nabla\boldsymbol{v}_h\right\|,$$

where P_h^{k-2} is the L^2 projection operator to the space of piecewise polynomials of degree no more than $k-2$. This completes the proof of (2.6).

By [6, Theorem 4.4.4] we have

$$\left\|(1-I_h)\boldsymbol{v}_h\right\|_{\infty,K} + h_K\left|(1-I_h)\boldsymbol{v}_h\right|_{1,\infty,K} \le Ch_K\left|\boldsymbol{v}_h\right|_{1,\infty,K}, \tag{4.11}$$

for all $K \in \mathcal{T}_h, \boldsymbol{v}_h \in V_h^0$. The inequality (2.7) follows immediately from a combination of the triangle inequality and (4.11).

For (2.8), similarly to (4.10), using (4.11) we have

$$\left\|\Pi_h^R\boldsymbol{v}_h\right\|_{\infty,K} \le C\left\|(1-I_h)\boldsymbol{v}_h\right\|_{\infty,K} \le Ch_K\left|\boldsymbol{v}_h\right|_{1,\infty,K}.$$

Thus we complete the proof. □

Up to now, we have proven that a class of divergence-free reconstruction operators satisfy the assumptions in Section 2.1. Thus it admits an a priori error estimate in Theorem 3.1. The only question is whether the right-hand side of (3.10) is an $O\left(h^k\right)$ quantity if $\boldsymbol{u}$ is sufficiently smooth. The non-trivial terms are the ones corresponding to $\Pi_h\boldsymbol{\eta}$ (including $E_d\left(\boldsymbol{\eta}\right)$), $\Pi_h^1\boldsymbol{\eta}$, $\Pi_h^R\boldsymbol{\eta}$ (including $E_d\left(\boldsymbol{\eta}\right)$ and $|||\boldsymbol{\eta}|||_*$) and $\|\Delta\boldsymbol{u}\circ\left(1-\Pi_h\right)\|_{\left(V_h^0\right)'}$. The following lemmas are to answer this question.

Lemma 6. *Let $\boldsymbol{u}$ be the solution of (2.10). Suppose that $\boldsymbol{u}\left(t\right)\in\boldsymbol{H}^{k+1}\left(\Omega\right)$ $\left(t\in J\right)$. Then we have*

$$\|\Delta\boldsymbol{u}\left(t\right)\circ\left(1-\Pi_h\right)\|_{\left(V_h^0\right)'}\leq Ch^k\left|\boldsymbol{u}\left(t\right)\right|_{k+1}. \tag{4.12}$$

Proof. The inequality (4.12) follows immediately from (2.6) by taking $\boldsymbol{g}=\Delta\boldsymbol{u}\left(t\right)$. □

Introduce the seminorm $|||\cdot|||_2$ on $\boldsymbol{H}^2\left(\mathcal{T}_h\right)$ by

$$|||\boldsymbol{v}|||_2^2:=\sum_{K\in\mathcal{T}_h}|\boldsymbol{v}|_{2,K}^2\quad\forall\ \boldsymbol{v}\in\boldsymbol{H}^2\left(\mathcal{T}_h\right).$$

Lemma 7. *Let $\boldsymbol{u}$ be the solution of (2.10) and $\boldsymbol{\eta}=\boldsymbol{u}-\Pi_h^S\boldsymbol{u}$. Suppose that $\boldsymbol{u}\in\boldsymbol{H}^{\frac{3}{2}+\epsilon}\left(\Omega\right)\cap\boldsymbol{H}^2\left(\mathcal{T}_h\right)$ with $\epsilon>0$. Then we have*

$$\|\Pi_h\boldsymbol{\eta}\|\leq\|\boldsymbol{\eta}\|+C\left(\|\boldsymbol{u}-I_h\boldsymbol{u}\|+\|\boldsymbol{\eta}\|+h^2|||\boldsymbol{\eta}|||_2\right), \tag{4.13}$$

$$\left\|\nabla\Pi_h^1\boldsymbol{\eta}\right\|\leq2\left\|\nabla\boldsymbol{\eta}\right\|+\left\|\nabla\left(\boldsymbol{u}-I_h\boldsymbol{u}\right)\right\|+Ch|||\boldsymbol{\eta}|||_2, \tag{4.14}$$

$$\left\|\Pi_h^R\boldsymbol{\eta}\right\|\leq C\left(\|\boldsymbol{u}-I_h\boldsymbol{u}\|+\|\boldsymbol{\eta}\|+h^2|||\boldsymbol{\eta}|||_2\right), \tag{4.15}$$

and

$$|||\boldsymbol{\eta}|||_*\leq C\left(\left\|\nabla\left(\boldsymbol{u}-I_h\boldsymbol{u}\right)\right\|+\|\nabla\boldsymbol{\eta}\|+h|||\boldsymbol{\eta}|||_2\right). \tag{4.16}$$

Proof. Note that

$$\begin{aligned}\Pi_h\boldsymbol{\eta}=\boldsymbol{u}-\Pi_h\Pi_h^S\boldsymbol{u}&=\boldsymbol{u}-I_h\Pi_h^S\boldsymbol{u}-\Pi_h^{RT}\left(1-I_h\right)\Pi_h^S\boldsymbol{u}\\&=\boldsymbol{\eta}+\left[\left(1-I_h\right)\Pi_h^S\boldsymbol{u}-\Pi_h^{RT}\left(1-I_h\right)\Pi_h^S\boldsymbol{u}\right],\end{aligned} \tag{4.17}$$

$$\Pi_h^1\boldsymbol{\eta}=\boldsymbol{u}-I_h\Pi_h^S\boldsymbol{u}=\boldsymbol{\eta}+\left(1-I_h\right)\Pi_h^S\boldsymbol{u}, \tag{4.18}$$

and

$$\Pi_h^R\boldsymbol{\eta}=-\Pi_h^R\Pi_h^S\boldsymbol{u}=-\Pi_h^{RT}\left(1-I_h\right)\Pi_h^S\boldsymbol{u}. \tag{4.19}$$

A common term in the right-hand sides of (4.17)-(4.19) is

$$\left(1-I_h\right)\Pi_h^S\boldsymbol{u}=\left(\boldsymbol{u}-I_h\boldsymbol{u}\right)+I_h\boldsymbol{\eta}. \tag{4.20}$$

Note that (4.3) guarantees with the triangle inequality

$$\|I_h\boldsymbol{v}\|_K\leq\|\boldsymbol{v}\|_K+Ch_K^2\left|\boldsymbol{v}\right|_{2,K}, \tag{4.21}$$

and

$$\|\nabla I_h\boldsymbol{v}\|_K\leq\|\nabla\boldsymbol{v}\|_K+Ch_K\left|\boldsymbol{v}\right|_{2,K}, \tag{4.22}$$

for all $\boldsymbol{v}\in\boldsymbol{C}^0\left(\bar{\Omega}\right)\cap\boldsymbol{H}^2\left(\mathcal{T}_h\right),K\in\mathcal{T}_h$. Substituting (4.21) and (4.22) into (4.20) gives

$$\left|\left(1-I_h\right)\Pi_h^S\boldsymbol{u}\right|_{m,K}\leq\left|\boldsymbol{u}-I_h\boldsymbol{u}\right|_{m,K}+\left|\boldsymbol{\eta}\right|_{m,K}+Ch_K^{2-m}\left|\boldsymbol{\eta}\right|_{2,K}\ \text{ for } m=0,1. \tag{4.23}$$

Substituting (4.23) into (4.17)-(4.19) and applying (4.6) for (4.17) and (4.19) provide (4.13)-(4.15).

To estimate $|||\boldsymbol{\eta}|||_*$, with (4.19), (4.6), (4.4) and the inverse inequality one obtains

$$\begin{aligned}\left\|\Pi_h^R\boldsymbol{\eta}\right\|_K \leq C\left\|(1-I_h)\,\Pi_h^S\boldsymbol{u}\right\|_K &\leq Ch_K^2\left|(1-I_h)\,\Pi_h^S\boldsymbol{u}\right|_{2,K}\\ &\leq Ch_K\left\|\nabla(1-I_h)\,\Pi_h^S\boldsymbol{u}\right\|_K.\end{aligned}$$

The above estimate, together with (3.7) and (4.23), implies that

$$|||\boldsymbol{\eta}|||_* \leq C\left\|\nabla(1-I_h)\,\Pi_h^S\boldsymbol{u}\right\| \leq C\left(\|\nabla(\boldsymbol{u}-I_h\boldsymbol{u})\|+\|\nabla\boldsymbol{\eta}\|+h|||\boldsymbol{\eta}|||_2\right).$$

This completes the proof. □

Finally, based on the results in Theorem 3.1, Lemma 6 and Lemma 7, as well as the approximation properties of I_h and Π_h^S [6, 23], we get the convergence rates of the kinetic and dissipation energy errors of $\boldsymbol{u}_h$ (or $\Pi_h\boldsymbol{u}_h$) for (2.13), with the elements and reconstruction operators in this section.

Corollary 1. *Let $(\boldsymbol{u},p)$ be the solution of (2.10) and $(\boldsymbol{u}_h,p_h)$ be the solution of (2.13), with the elements and reconstruction operators used in Section 4. Suppose $\boldsymbol{u}\in L^\infty\left(J;\boldsymbol{H}^{k+1}(\Omega)\right)\cap L^2\left(J;\boldsymbol{W}^{1,\infty}(\Omega)\right)$, $\boldsymbol{u}_t\in L^2\left(J;\boldsymbol{H}^{k+1}(\Omega)\right)$. Under Assumption 3 and the assumption that $\boldsymbol{u}_h^0=\Pi_h^S\boldsymbol{u}^0$, the following estimate holds:*

$$\|\boldsymbol{u}-\boldsymbol{u}_h\|_{L^\infty(J;\boldsymbol{L}^2(\Omega))}+\nu^{\frac{1}{2}}\|\nabla(\boldsymbol{u}-\boldsymbol{u}_h)\|_{L^2(J;\boldsymbol{L}^2(\Omega))}\leq B(\boldsymbol{u},T)\,h^k, \tag{4.24}$$

where

$$\begin{aligned}B(\boldsymbol{u},T)=C\Big\{&h\,|\boldsymbol{u}|_{L^\infty\left(J;\boldsymbol{H}^{k+1}(\Omega)\right)}+|\boldsymbol{u}|_{L^2\left(J;\boldsymbol{H}^{k+1}(\Omega)\right)}+e^{\frac{1}{2}G(\boldsymbol{u},T)}\Big[\\ &h\,|\boldsymbol{u}_t|_{L^2\left(J;\boldsymbol{H}^{k+1}(\Omega)\right)}+|\boldsymbol{u}|_{L^2\left(J;\boldsymbol{H}^{k+1}(\Omega)\right)}+\|\boldsymbol{u}\|_{L^2(J;\boldsymbol{W}^{1,\infty}(\Omega))}\,|\boldsymbol{u}|_{L^4\left(J;\boldsymbol{H}^{k+1}(\Omega)\right)}\Big]\Big\},\end{aligned}$$

with C independent of p, h and inverse powers of ν.

5. Numerical experiments

5.1. **Example 1: convergence test and pressure-robustness test.** For the first example we consider the potential flow in [37, Example 6]. On $\Omega=(0,1)^2$ the velocity is prescribed as $\boldsymbol{u}=\min\{t,1\}\nabla\chi$ with $\chi=x^3y-y^3x$. We set $\boldsymbol{f}=0$ such that the pressure gradient exactly balances the gradient filed produced by the velocity terms. Due to the quadratic convective term, the pressure is much more complicated than the velocity [21]. The pressure-robustness will paly a key role on the accuracy of the simulations of this problem. We use this example to show the convergence rates and the pressure-robustness of our method.

We consider the case of $\nu=5\times10^{-4}$ and apply the first order Bernardi-Raugel element and the second order element mentioned in Section 4, P_2^{bubble}/P_1^{disc}. For the time-stepping, the BDF2 scheme is used. For convergence test, here we only consider the spatial effects and neglect the effects of the time discretizations by choosing a small time step: $\Delta t=0.001$ and $T=0.1$. A non-uniform initial mesh is used, which consists of 132 triangles and produces total 506 DOFs for Bernardi-Raugel element and 1246 DOFs for P_2^{bubble}/P_1^{disc}. The pressure-robustness test is performed on the double refinement of the initial mesh, with the time step $\Delta t=0.01$ and $T=2$. We also give some results from the classical scheme and the pressure-robust reconstruction scheme in [37] with the convective form for the nonlinear

TABLE 2. Example 1. Errors by the Bernardi-Raugel element with $\alpha = 0, T = 0.1$.

level	$\|\boldsymbol{u} - \boldsymbol{u}_h\|$	eoc	$\|\boldsymbol{u} - \Pi_h\boldsymbol{u}_h\|$	eoc	$\|\nabla(\boldsymbol{u} - \boldsymbol{u}_h)\|$	eoc	$\|p - p_h\|$	eoc
0	4.3762e-4	–	5.5822e-4	–	2.7562e-2	–	2.2363e-2	–
1	1.0781e-4	2.02	1.4006e-4	1.99	1.3462e-2	1.03	1.1242e-2	0.99
2	2.6214e-5	2.04	3.4968e-5	2.00	6.5417e-3	1.04	5.6197e-3	1.00
3	6.4910e-6	2.01	8.7537e-6	1.99	3.2321e-3	1.01	2.8093e-3	1.00

TABLE 3. Example 1. Errors by P_2^{bubble}/P_1^{disc} with $\alpha = 0, T = 0.1$.

level	$\|\boldsymbol{u} - \boldsymbol{u}_h\|$	eoc	$\|\boldsymbol{u} - \Pi_h\boldsymbol{u}_h\|$	eoc	$\|\nabla(\boldsymbol{u} - \boldsymbol{u}_h)\|$	eoc	$\|p - p_h\|$	eoc
0	1.1624e-5	–	1.4688e-5	–	9.4495e-4	–	1.2894e-3	–
1	1.4175e-6	3.03	1.9025e-6	2.94	2.2039e-4	2.10	3.2351e-4	1.99
2	1.8333e-7	2.95	2.4828e-7	2.93	5.4150e-5	2.02	8.0835e-5	2.00
3	2.3777e-8	2.94	3.2014e-8	2.95	1.3519e-5	2.00	2.0233e-5	1.99

TABLE 4. Example 1. Errors by the Bernardi-Raugel element with $\alpha = 1, T = 0.1$.

level	$\|\boldsymbol{u} - \boldsymbol{u}_h\|$	eoc	$\|\boldsymbol{u} - \Pi_h\boldsymbol{u}_h\|$	eoc	$\|\nabla(\boldsymbol{u} - \boldsymbol{u}_h)\|$	eoc	$\|p - p_h\|$	eoc
0	4.7428e-4	–	5.7279e-4	–	2.8068e-2	–	2.2364e-2	–
1	1.0993e-4	2.10	1.4107e-4	2.02	1.3287e-2	1.07	1.1242e-2	0.99
2	2.6469e-5	2.05	3.5056e-5	2.00	6.5124e-3	1.02	5.6197e-3	1.00
3	6.5237e-6	2.02	8.7597e-6	2.00	3.2315e-3	1.01	2.8093e-3	1.00

term. In each time step, we solve a linear problem by replacing the advective velocity in trilinear forms with some appropriate extrapolation of the previous step velocities.

Finally, to show the pressure-robustness of our methods further, we also compute the problem with $\boldsymbol{f} = 100\nabla\chi$, which only change the pressure in the continuous problem and the discrete pressure for pressure-robust methods. Some results are shown in Tables 2 to 8. For pressure-robust tests, we only show the results with $\alpha = 0$. The results below, especially the results in Table 8, demonstrate that our methods are robust with respect to the continuous pressure.

For second order tests, we find that our methods give a little worse result than the pressure-robust reconstruction methods in [37]. This is reasonable since we alter the discretization of the convective form. Although our methods are EMA-conserving, these advantages is not easy to shown in a potential flow unless we use a much smaller viscosity.

5.2. **Example 2: EMA-conserving test: the Gresho problem.** In the second example we consider the Gresho problem [10, 11, 21], which is a benchmark to test the EMA-conserving properties of a method. With $\boldsymbol{f} = \boldsymbol{0}$ and $\nu = 0$, the exact solutions on $\Omega = (-0.5, 0.5)^2$ are set as

$$r \le 0.2 : \begin{cases} \boldsymbol{u} = \begin{pmatrix} -5y \\ 5x \end{pmatrix}, \\ p = 12.5r^2 + \gamma \end{cases} \quad 0.2 \le r \le 0.4 : \begin{cases} \boldsymbol{u} = \begin{pmatrix} -\frac{2y}{r} + 5y \\ \frac{2x}{r} - 5x \end{pmatrix}, \\ p = 12.5r^2 - 20r + 4\log(r) + \beta \end{cases}$$

TABLE 5. Example 1. Errors by P_2^{bubble}/P_1^{disc} with $\alpha = 1, T = 0.1$.

level	$\|\boldsymbol{u}-\boldsymbol{u}_h\|$	eoc	$\|\boldsymbol{u}-\Pi_h\boldsymbol{u}_h\|$	eoc	$\|\nabla(\boldsymbol{u}-\boldsymbol{u}_h)\|$	eoc	$\|p-p_h\|$	eoc
0	1.2393e-5	–	1.6257e-5	–	9.1896e-4	–	1.2894e-3	–
1	1.4720e-6	3.07	2.0064e-6	3.01	2.1807e-4	2.07	3.2351e-4	1.99
2	1.8534e-7	2.98	2.5244e-7	2.99	5.4057e-5	2.01	8.0835e-5	2.00
3	2.3864e-8	2.95	3.2125e-8	2.97	1.3523e-5	1.99	2.0233e-5	1.99

TABLE 6. Example 1. Errors by the Bernardi-Raugel element with $\alpha = 0$ on mesh level 2 (classical methods/EMAPR/pressure-robust reconstructions).

t	$\|\boldsymbol{u}-\boldsymbol{u}_h\|$	$\|\nabla(\boldsymbol{u}-\boldsymbol{u}_h)\|$	$\|P_hp-p_h\|$
0.5	1.84e-2/1.61e-4/1.62e-4	3.66/3.72e-2/3.86e-2	1.63e-2/5.02e-5/4.70e-5
1	4.35e-2/4.47e-4/4.71e-4	8.47/8.73e-2/9.83e-2	5.59e-2/2.46e-4/2.29e-4
1.5	5.50e-2/5.56e-4/6.07e-4	9.24/8.89e-2/0.10	4.02e-2/2.62e-4/2.37e-4
2.0	5.53e-2/5.98e-4/7.37e-4	9.24/8.90e-2/0.10	4.09e-2/2.84e-4/2.68e-4

TABLE 7. Example 1. Errors by P_2^{bubble}/P_1^{disc} with $\alpha = 0$ on mesh level 2 (classical methods/EMAPR/pressure-robust reconstructions).

t	$\|\boldsymbol{u}-\boldsymbol{u}_h\|$	$\|\nabla(\boldsymbol{u}-\boldsymbol{u}_h)\|$	$\|P_hp-p_h\|$
0.5	4.85e-5/1.61e-6/1.20e-6	1.21e-2/4.55e-4/3.36e-4	6.94e-5/1.09e-6/5.80e-7
1	9.81e-5/4.95e-6/3.40e-6	2.58e-2/1.34e-3/8.69e-4	1.50e-4/5.14e-6/2.54e-6
1.5	1.15e-4/5.75e-6/3.80e-6	2.65e-2/1.36e-3/8.95e-4	1.44e-4/5.29e-6/2.64e-6
2.0	1.17e-4/6.07e-6/3.94e-6	2.66e-2/1.37e-3/8.98e-4	1.43e-4/5.47e-6/2.73e-6

TABLE 8. Example 1. Errors with $\alpha = 0$ and $\boldsymbol{f} = 100\nabla\chi$ on mesh level 2 (classical methods/EMAPR).

	Bernardi-Raugel		P_2^{bubble}/P_1^{disc}	
t	$\|\boldsymbol{u}-\boldsymbol{u}_h\|$	$\|\nabla(\boldsymbol{u}-\boldsymbol{u}_h)\|$	$\|\boldsymbol{u}-\boldsymbol{u}_h\|$	$\|\nabla(\boldsymbol{u}-\boldsymbol{u}_h)\|$
0.5	1.51/1.61e-4	265.73/3.72e-2	4.80e-3/1.61e-6	1.10/4.55e-4
1	1.62/4.47e-4	285.33/8.73e-2	3.74e-3/4.95e-6	0.90/1.34e-3
1.5	1.74/5.56e-4	284.10/8.89e-2	3.78e-3/5.75e-6	0.90/1.36e-3
2	1.78/5.98e-4	280.08/8.90e-2	3.86e-3/6.07e-6	0.90/1.37e-3

and all vanish for $r > 0.4$, where $r = \sqrt{x^2+y^2}$ and

$$\beta = (-12.5)(0.4)^2 + 20(0.4)^2 - 4\log(0.4), \gamma = \beta - 20(0.2) + 4\log(0.2).$$

We strongly enforce the no-penetration boundary condition in computations. And set $\alpha = 0$ and $\alpha = 1$ for Bernardi-Raugel element and P_2^{bubble}/P_1^{disc}, respectively. We find that for this problem the gradient of the velocity solution might be very large for higher order elements ($k \geq 2$) if $\alpha = 0$. This is the reason for the choice of α. The Bernardi-Raugel element is tested on a uniform 48×48 triangular mesh and the P_2^{bubble}/P_1^{disc} is tested on a non-uniform mesh with $h = 1/25$. To

highlight the conservative properties, we apply the Crank-Nicolson scheme for time discretizations with $\Delta t = 0.01$ and $T = 10$.

To make a comparison, we also compute the results from two classes of conservative methods: one is the EMAC formulation [10, 42] with the same elements and meshes as our methods, the other is the classical convective formulation but with the exactly divergence-free elements. For the first order divergence-free elements, we choose the element proposed by Guzmán and Neilan in [27], which is performed on the same mesh as the Bernardi-Raugel element. Note that the Guzmán-Neilan element has the same DOFs as the Bernardi-Raugel element on a given mesh. The Guzmán-Neilan element consists of linear pieceewise polynomials and some modified Bernardi-Raugel bubbles which are constructed on the barycentric refinement of each triangle. For the second order divergence-free elements, we choose the well-known Scott-Vogelius (SV2) element, P_2/P_1^{disc} [3, 30], which is run on the barycentric refinement of the mesh for P_2^{bubble}/P_1^{disc} to guarantee the stability. For all methods we solve a nonlinear system in each step by Newton iterations or Picard iterations with a tolerance of 10^{-6} for H^1 norm.

Some results are shown in Fig. 1 and Fig. 2, where the "momentum" denotes the sum of all the components of the linear momentum. For EMAPR methods, all the quantities are computed by $\Pi_h \boldsymbol{u}_h$. For first order approximations, the pressure is approximated by piecewise constant. In this time, the effect of the lack of pressure-robustness for the EMAC formulation is obvious. For higher order approximations, all the methods give very similar results, since the continuous pressure is not very complicated (the maximum power is 2) and all the methods are EMA-conserving.

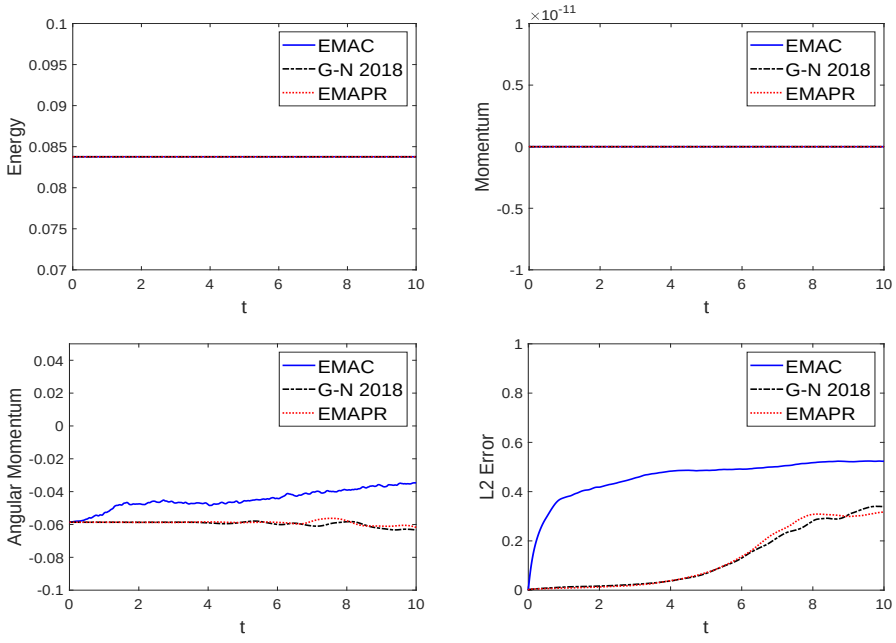


FIGURE 1. Example 2. Plots of kinetic energy, momentum, angular momentum and L2 errors by the Bernardi-Raugel element or Guzmán-Neilan element (G-N 2018) versus time.

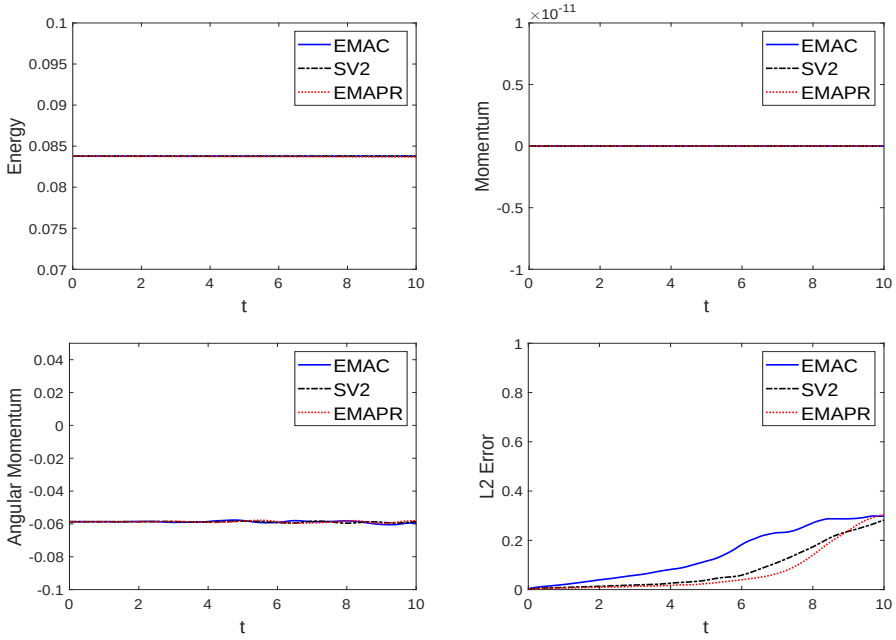


FIGURE 2. Example 2. Plots of kinetic energy, momentum, angular momentum and L2 errors by P_2^{bubble}/P_1^{disc} or SV2 versus time.

5.3. **Example 3: Re-semi-robustness test: the lattice vortex problem.** In the final example, we consider the lattice vortex problem [42, 46] on $\Omega = (0,1)^2$, which is a benchmark to test the exponential growth rates (with respect to time) of the errors. In Section 4 we have shown that the Gronwall constant is independent of ν. The exact velocity is set as $\boldsymbol{u}(t,\boldsymbol{x}) = \boldsymbol{u}^0(\boldsymbol{x})\exp\left(-8\pi^2\nu t\right)$ with $\boldsymbol{u}^0(\boldsymbol{x}) = (\sin(2\pi x)\sin(2\pi y), \cos(2\pi x)\cos(2\pi y))^{\mathrm{T}}$. With an appropriate p, $\boldsymbol{u}$ fulfills an exact unsteady NSE with $\boldsymbol{f} = \boldsymbol{0}$. To test the Re-semi-robustness, we choose a small ν and large T: $\nu = 1\times 10^{-5}$ and $T = 10$.

The methods (or elements) used in this example are the same as Section 5.2, except replacing the EMAC scheme with the classical skew-symmetric scheme (SKEW), which has been shown not to be Re-semi-robust with non-divergence-free elements [42, 46]. All the first order methods are run on the uniform 64×64 triangular mesh. The P_2^{bubble}/P_1^{disc} are tested on a non-uniform mesh with the size $h = 0.03$, and the SV2 element is performed on the barycentric refinement of the same mesh. For our methods, we give the results for both $\alpha = 0$ and $\alpha = 1$. Note that from the theoretical analysis the value of α has an effect on the property of Re-semi-robustness. For the time discretizations, we use the Crank-Nicolson scheme with $\Delta t = 0.001$. We linearize all the methods by replacing the first velocity in trilinear forms with some appropriate extrapolation of the previous step velocities.

Some results are shown in Figs. 3 and 4. One could find that the value of α does have an effect on the growth speed of the errors. For first order approximations, the methods (elements) proposed by Guzmán and Neilan in [27] give the best results,

and our method with $\alpha = 1$ gives very close performance in the final time. For second order approximations, our method admits the best performance. Except the SKEW formulation on non-divergence-free elements, all the methods below show a slower growth speed of the errors.

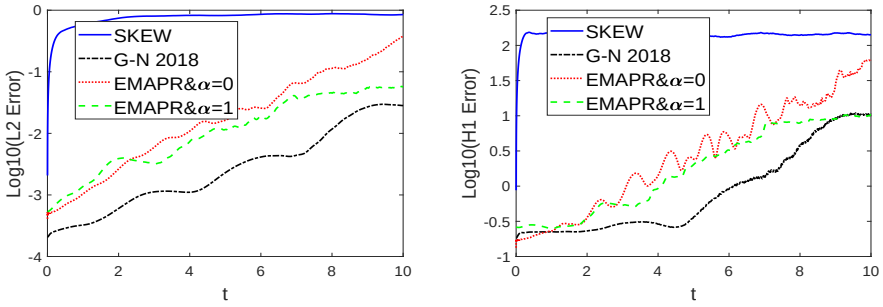


FIGURE 3. Example 3. Plots of L2 errors, H1 errors by the Bernardi-Raugel element or Guzmán-Neilan element versus time.

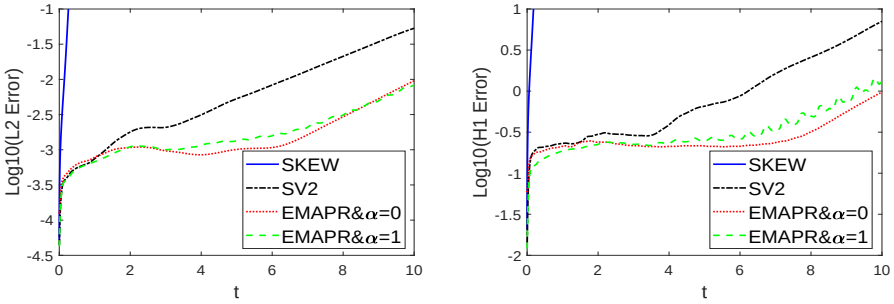


FIGURE 4. Example 3. Plots of L2 errors, H1 errors by P_2^{bubble}/P_1^{disc} or SV2 versus time.

REFERENCES

1. R.V. Abramov and A.J. Majda, *Discrete approximations with additional conserved quantities: deterministic and statistical behavior*, Methods Appl. Anal. **10** (2003), no. 2, 151–190. 1
2. Akio Arakawa, *Computational design for long-term numerical integration of the equations of fluid motion: Two dimensional incompressible flow, Part I*, J. Comput. Phys. **1** (1966), 119–143. 1
3. D. N. Arnold and J. Qin, *Quadratic velocity/linear pressure Stokes elements*, Advances in Computer Methods for Partial Differential Equations-VII, R. Vichnevetsky, D. Knight & G. Richter, eds., IMACS, New Brunswick, NJ (1992), 28–34. 5.2
4. Christine Bernardi and Genevieve Raugel, *Analysis of some finite elements for the Stokes problem*, Math. Comp. **44** (1985), no. 169, 71–79. 4
5. Daniele Boffi, Franco Brezzi, and Michel Fortin, *Mixed finite element methods and applications*, Springer Series in Computational Mathematics, vol. 44, Springer Berlin Heidelberg, 2013. 4, 4, 4
6. Susanne C. Brenner and L. Ridgway Scott, *The mathematical theory of finite element methods*, Texts in Applied Mathematics, vol. 15, Springer New York, New York, NY, 2008. 4, 4, 4, 4

7. F. Brezzi, T. J. R. Hughes, L. D. Marini, and A. Masud, *Mixed discontinuous Galerkin methods for Darcy flow*, J. Sci. Comput. **22-23** (2005), no. 1-3, 119–145. 3
8. Erik Burman and Miguel A. Fernández, *Continuous interior penalty finite element method for the time-dependent Navier-Stokes equations: space discretization and convergence*, Numer. Math. **107** (2007), no. 1, 39–77. 1
9. Michael A. Case, Vincent J. Ervin, Alexander Linke, and Leo G. Rebholz, *A connection between Scott-Vogelius and grad-div stabilized Taylor-Hood FE approximations of the Navier-Stokes equations*, SIAM J. Numer. Anal. **49** (2011), no. 4, 1461–1481. 1
10. Sergey Charnyi, Timo Heister, Maxim A. Olshanskii, and Leo G. Rebholz, *On conservation laws of Navier-Stokes Galerkin discretizations*, J. Comput. Phys. **337** (2017), 289–308. 1, 2.2, 2.3, 2.3, 4, 5.2
11. Sergey Charnyi, Timo Heister, Maxim A. Olshanskii, and Leo G. Rebholz, *Efficient discretizations for the EMAC formulation of the incompressible Navier-Stokes equations*, Appl. Numer. Math. **141** (2019), 220–233. 1, 2.3, 5.2
12. Snorre H. Christiansen and Kaibo Hu, *Generalized finite element systems for smooth differential forms and Stokes' problem*, Numer. Math. **140** (2018), no. 2, 327–371. 1
13. Philippe G. Ciarlet, *The finite element method for elliptic problems*, Society for Industrial and Applied Mathematics, 2002. 2.1
14. Bernardo Cockburn, Guido Kanschat, and Dominik Schötzau, *A note on discontinuous Galerkin divergence-free solutions of the Navier-Stokes equations*, J. Sci. Comput. **31** (2007), no. 1-2, 61–73. 1
15. Javier de Frutos, Bosco García-Archilla, Volker John, and Julia Novo, *Analysis of the grad-div stabilization for the time-dependent Navier-Stokes equations with inf-sup stable finite elements*, Adv. Comput. Math. **44** (2018), no. 1, 195–225. 1
16. ———, *Error analysis of non inf-sup stable discretizations of the time-dependent Navier-Stokes equations with local projection stabilization*, IMA J. Numer. Anal. **39** (2019), no. 4, 1747–1786. 1
17. Daniele Antonio Di Pietro and Alexandre Ern, *Mathematical aspects of discontinuous Galerkin methods*, Mathematiques et Applications, vol. 69, Springer Berlin Heidelberg, Berlin, Heidelberg, 2012. 2.3
18. John A. Evans and Thomas J. R. Hughes, *Isogeometric divergence-conforming B-splines for the unsteady Navier-Stokes equations*, J. Comput. Phys. **241** (2013), 141–167. 1
19. George J. Fix, *Finite Element Models for Ocean Circulation Problems*, SIAM J. Appl. Math. **29** (1975), no. 3, 371–387. 1
20. Bosco García-Archilla, Volker John, and Julia Novo, *Symmetric pressure stabilization for equal-order finite element approximations to the time-dependent Navier-Stokes equations*, IMA J. Numer. Anal. **41** (2021), no. 2, 1093–1129. 1
21. Nicolas R. Gauger, Alexander Linke, and Philipp W. Schroeder, *On high-order pressure-robust space discretisations, their advantages for incompressible high Reynolds number generalised Beltrami flows and beyond*, The SMAI journal of computational mathematics **5** (2019), 89–129. 5.1, 5.2
22. V. Girault, R. H. Nochetto, and L. R. Scott, *Max-norm estimates for Stokes and Navier-Stokes approximations in convex polyhedra*, Numer. Math. **131** (2015), no. 4, 771–822. 3
23. Vivette Girault and Pierre-Arnaud Raviart, *Finite element methods for Navier-Stokes equations*, Springer Series in Computational Mathematics, vol. 5, Springer Berlin Heidelberg, Berlin, Heidelberg, 1986. 1, 2.2, 4, 4
24. Johnny Guzmán and Michael Neilan, *A family of nonconforming elements for the Brinkman problem*, IMA J. Numer. Anal. **32** (2012), no. 4, 1484–1508. 1
25. ———, *Conforming and divergence-free Stokes elements on general triangular meshes*, Math. Comp. **83** (2013), no. 285, 15–36. 1
26. Johnny Guzmán and Michael Neilan, *Conforming and divergence-free Stokes elements in three dimensions*, IMA J. Numer. Anal. **34** (2014), 1489–1508. 1
27. Johnny Guzmán and Michael Neilan, *Inf-sup stable finite elements on barycentric refinements producing divergence–free approximations in arbitrary dimensions*, SIAM J. Numer. Anal. **56** (2018), no. 5, 2826–2844. 1, 5.2, 5.3
28. Volker John, *Finite element methods for incompressible flow problems*, Springer, New York, 2016. 1

29. Volker John, Petr Knobloch, and Julia Novo, *Finite elements for scalar convection-dominated equations and incompressible flow problems: a never ending story?*, Comput. Visual Sci. **19** (2018), no. 5-6, 47–63. 1
30. Volker John, Alexander Linke, Christian Merdon, Michael Neilan, and Leo G. Rebholz, *On the divergence constraint in mixed finite element methods for incompressible flows*, SIAM Rev. **59** (2017), no. 3, 492–544. 1, 5.2
31. Juho Könnö and Rolf Stenberg, *H(div)-conforming finite elements for the Binkman problem*, Math. Models Methods Appl. Sci. **21** (2011), no. 11, 2227–2248. 1
32. Philip L. Lederer, *Pressure-robust discretizations for Navier-Stokes equations: Divergence-free reconstruction for Taylor-Hood elements and high order hybrid discontinuous Galerkin methods*, Master's thesis, Vienna Technical University, Vienna, 2016. 1
33. Philip L. Lederer, Christoph Lehrenfeld, and Joachim Schöberl, *Hybrid discontinuous Galerkin methods with relaxed H(div)-conformity for incompressible flows. Part II*, ESAIM: Math. Model. Numer. Anal. **53** (2019), no. 2, 503–522. 1
34. Philip L. Lederer, Alexander Linke, Christian Merdon, and Joachim Schöberl, *Divergence-free reconstruction operators for pressure-robust Stokes discretizations with continuous pressure finite elements*, SIAM J. Numer. Anal. **55** (2017), no. 3, 1291–1314. 1, 2
35. Alexander Linke, *On the role of the Helmholtz decomposition in mixed methods for incompressible flows and a new variational crime*, Comput. Methods Appl. Mech. Engrg. **268** (2014), 782–800. 1
36. Alexander Linke, Gunar Matthies, and Lutz Tobiska, *Robust arbitrary order mixed finite element methods for the incompressible Stokes equations with pressure independent velocity errors*, ESAIM: Math. Model. Numer. Anal. **50** (2016), no. 1, 289–309. 1, 3, 4
37. Alexander Linke and Christian Merdon, *Pressure-robustness and discrete Helmholtz projectors in mixed finite element methods for the incompressible Navier-Stokes equations*, Comput. Methods Appl. Mech. Engrg. **311** (2016), 304–326. 1, 2.1, 2.2, 3, 3, 4, 5.1
38. Alexander Linke and Leo G. Rebholz, *Pressure-induced locking in mixed methods for time-dependent Navier-Stokes equations*, J. Comput. Phys. **388** (2019), 350–356. 1
39. Michael Neilan, *Discrete and conforming smooth de Rham complexes in three dimensions*, Math. Comp. **84** (2015), 2059–2081. 1
40. Michael Neilan and Baris Otus, *Divergence-free Scott–Vogelius elements on curved domains*, SIAM J. Numer. Anal. **59** (2021), no. 2, 1090–1116. 1
41. M. A. Olshanskii and A. Reusken, *Grad-div stabilization for Stokes equations*, Math. Comp. **73** (2004), 1699–1718. 1
42. Maxim A. Olshanskii and Leo G. Rebholz, *Longer time accuracy for incompressible Navier-Stokes simulations with the EMAC formulation*, Comput. Methods Appl. Mech. Engrg. **372** (2020), 113369. 1, 2.3, 3, 5.2, 5.3
43. A. Palha and M. Gerritsma, *A mass, energy, enstrophy and vorticity conserving (MEEVC) mimetic spectral element discretization for the 2D incompressible Navier-Stokes equations*, J. Comput. Phys. **328** (2017), 200–220. 1
44. Leo G. Rebholz, *An energy- and helicity-conserving finite element scheme for the Navier-Stokes equations*, SIAM J. Numer. Anal. **45** (2007), no. 4, 1622–1638. 1
45. Sander Rhebergen and Garth N. Wells, *An embedded-hybridized discontinuous Galerkin finite element method for the Stokes equations*, Comput. Methods Appl. Mech. Engrg. **358** (2020), 112619. 1
46. Philipp W. Schroeder, Christoph Lehrenfeld, Alexander Linke, and Gert Lube, *Towards computable flows and robust estimates for inf-sup stable FEM applied to the time-dependent incompressible Navier-Stokes equations*, SeMA **75** (2018), no. 4, 629–653. 1, 3, 5.3
47. Junping Wang, Xiaoshen Wang, and Xiu Ye, *Finite element methods for the Navier-Stokes equations by H(div) elements*, J. Comput. Math. **26** (2008), 410–436. 1
48. Junping Wang and Xiu Ye, *New finite element methods in computational fluid dynamics by H(div) elements*, SIAM J. Numer. Anal. **45** (2007), no. 3, 1269–1286. 1
49. Shangyou Zhang, *A new family of stable mixed finite elements for the 3D Stokes equations*, Math. Comp. **74** (2005), no. 250, 543–554. 1

School of Mathematics, Shandong University, Jinan 250100, China
Email address: xulisdu@126.com

School of Mathematics, Shandong University, Jinan 250100, China
Email address: hxrui@sdu.edu.cn